Illinois Basin – Decatur Project: Soil Carbon Dioxide Flux Monitoring

Carl H. Carman, Curt S. Blakley, Christopher P. Korose, and Randall A. Locke II

Illinois State Geological Survey, Prairie Research Institute, University of Illinois at Urbana-Champaign

Circular 599 2019

ILLINOIS STATE GEOLOGICAL SURVEY
Prairie Research Institute
University of Illinois at Urbana-Champaign

ILLINOIS
Illinois State Geological Survey
PRAIRIE RESEARCH INSTITUTE

Front cover: *(Top left) Field data being recorded during a flux measurement; (top right) deployed multiplexer accumulation chambers; (bottom left) a natural-shallow ring installation; (bottom right) LI-8100A analyzer control unit and accumulation chamber during field use at a bare-shallow installation.*

Illinois Basin – Decatur Project: Soil Carbon Dioxide Flux Monitoring

Carl H. Carman, Curt S. Blakley, Christopher P. Korose, and Randall A. Locke II

Illinois State Geological Survey, Prairie Research Institute, University of Illinois at Urbana-Champaign

Circular 599 2019

ILLINOIS STATE GEOLOGICAL SURVEY
Prairie Research Institute
University of Illinois at Urbana-Champaign
615 E. Peabody Drive
Champaign, Illinois 61820-6918
http://www.isgs.illinois.edu

ILLINOIS
Illinois State Geological Survey
PRAIRIE RESEARCH INSTITUTE

Suggested citation:
Carman, C.H., C.S. Blakley, C.P. Korose, and R.A. Locke II, 2019, Illinois Basin – Decatur Project: Soil carbon dioxide flux monitoring: Illinois State Geological Survey, Circular 599, 27 p.

Contents

Tables

Figures

EXECUTIVE SUMMARY

The purpose of this report is to provide a summary of soil carbon dioxide flux measurements collected at the Illinois Basin – Decatur Project (IBDP). The IBDP is a geologic carbon storage project that successfully injected 1 million tonnes (1.1 million tons) of carbon dioxide (CO_2) into the Mt. Simon Sandstone at an industrial site in Decatur, Illinois. Injection began on November 17, 2011, and concluded on November 26, 2014. The IBDP monitoring, verification, and accounting (MVA) program included a soil CO_2 flux monitoring network that used the closed-chamber accumulation method to estimate fluxes in the study area on an approximately weekly basis from June 2009 to June 2015. The 109 discrete monitoring installations in the network were designed to examine the effects of vegetation removal and ring insertion depth (8 vs. 46 cm, or 3.1 vs. 18.1 in.) on the magnitude and variability of fluxes. The network consisted of three installation types: (1) bare-shallow, (2) natural-shallow, and (3) bare-deep. Bare-shallow and bare-deep installations were inserted to 8 and 46 cm (3.1 and 18.1 in.), respectively, below the soil surface, and herbicide was applied around these two installation types to minimize the contribution of vegetation to soil CO_2 fluxes. Natural-shallow installations were inserted to 8 cm (3.1 in.) below the soil surface, and vegetation was trimmed only when necessary to allow a flux measurement to be taken. Soil temperature and moisture data were collected simultaneously with flux measurements when possible to examine their relationship to fluxes. Soil temperatures were compared with local air temperatures measured at the Decatur airport, and when soil temperature data were not able to be collected, air temperatures were determined to be a satisfactory proxy. In total, 12,904 flux measurements were collected during the project. Nonparametric statistics were used to test fluxes measured at each location to evaluate whether CO_2 injection activities had affected fluxes at the IBDP site. Overall, our statistical examination of the flux data indicated that soil CO_2 fluxes at the IBDP site were not affected by CO_2 injection.

Soil CO_2 fluxes varied with seasonal temperature cycles, as expected. Extremes in soil moisture affected the soil CO_2 fluxes; for example, a drought in 2012 caused fluxes from April to July to be 37% lower than the site average for that period across all monitoring years. Fluxes at the bare-shallow installations ranged from 1.3 ± 1.0 to 1.8 ± 1.3 μmol $m^{-2}s^{-1}$, and those at the bare-deep installations ranged from 1.4 ± 1.5 to 1.8 ± 1.7 μmol $m^{-2}s^{-1}$. Fluxes at the natural-shallow installations ranged from 4.2 ± 3.7 to 5.3 ± 3.6 μmol $m^{-2}s^{-1}$. The IBDP benefited from the development of such a comprehensive data set, although similar high-density, high-frequency monitoring protocols may not be practical for larger scale demonstration and commercial projects. The IBDP network was not expected to provide a protocol for how to deploy soil flux monitoring, but rather to provide a detailed understanding of flux behaviors at one site so that those experiences could be used to guide the development of monitoring programs at other carbon capture and storage sites. Fluxes at the bare-shallow installations were smaller and less variable than those at the natural-shallow installations and would be more effective in identifying a surface leak signature if one were to occur. Therefore, the bare-shallow installation is suggested as the preferred type for monitoring soil CO_2 fluxes at an industrial carbon capture and storage site. However, we recognize that this type of installation (e.g., one with periodic herbicide treatment) may not be practical for all sites. Measurements from a natural-shallow installation would also likely be able to detect leaks, but this type of installation could be more difficult to use because of the added CO_2 flux variability of natural vegetation. In the closed-chamber method, flux measurements rely on gas exchange across the soil–atmosphere boundary, but freezing temperatures often prevented this gas exchange, which is a significant drawback to this monitoring technique. The closed-chamber method can be used to provide estimates of leak quantification, but given the anticipated nature of leaks (e.g., diffuse, with small surface expression, possibly sporadic, with potentially low flux rates compared with the range of natural variability, and having potential surface expression as methane), soil flux was not used as a primary indicator of leakage at the IBDP. Instead, it was used as a point of reference to define flux variability over the life of the project should significant anomalous signals be observed. For researchers who wish to conduct further analyses, soil CO_2 flux data collected at the IBDP from 2009 to 2015 are available in electronic format on request.

INTRODUCTION

The release of carbon dioxide (CO_2) into the atmosphere occurs through both natural processes and anthropogenic activities, such as fossil fuel combustion. The amount of CO_2, which acts as a greenhouse gas, is positively correlated with global temperature increases (Intergovernmental Panel on Climate Change 2014). The risks and costs presented by increasing concentrations of greenhouse gases in the atmosphere have driven the research and development of processes such as carbon capture and sequestration (CCS), which has the potential to significantly reduce anthropogenic CO_2 emissions and thus help mitigate the effects of global climate change.

The Midwest Geological Sequestration Consortium (MGSC) is one of seven Regional Carbon Sequestration Partnerships created by the U.S. Department of Energy and funded by the National Energy Technology Laboratory to advance carbon storage technologies nationwide (MGSC 2017). One of the major projects conducted by the MGSC is the Illinois Basin – Decatur Project (IBDP), a collaboration of the Illinois State Geological Survey, the Archer Daniels Midland Company (ADM), Schlumberger Carbon Services, and other participants. The IBDP is a large-scale demonstration project involving geologic storage of 1 million tonnes (1.1 million tons) of CO_2 over a 3-year injection period. High-purity (>99%) CO_2 was captured during the corn fermentation process used to produce ethanol at ADM's corn-processing plant in Decatur, Illinois (Figure 1), and then dehydrated, compressed, and transported by a 1.9-km (1.2-mi) pipeline to the injection well (CCS1). Carbon dioxide injection began on November 4, 2011, reached full 24-hour operation by November 17, 2011, and was completed successfully on November 26, 2014, with a total mass of 999,215 tonnes (1,101,446 tons) stored.

The extensive IBDP monitoring, verification, and accounting (MVA) program used multiple monitoring methods to

Figure 1 Location of the Illinois Basin – Decatur Project (IBDP) in relation to the Illinois Basin (green area).

(1) establish environmental baseline site conditions, (2) detect significant environmental impacts of CO_2 injection, (3) demonstrate that project activities were protective of human health and the environment, and (4) provide an accurate accounting of stored CO_2 (Table 1). The purpose of this report is to summarize results from the soil CO_2 flux monitoring network and associated information collected from June 2009 to July 2015. Researchers can request the compiled and quality-controlled flux data in digital format should they wish to use it (see Accompanying Digital Data section on p. 22).

The soil CO_2 flux monitoring network was developed to characterize the magnitude and variability of pre-CO_2 injection soil CO_2 fluxes at the IBDP site and use that information to find and quantify a leak if one were to occur. Extensive spatial and temporal baseline flux data were collected and used to analyze injection-period and postinjection-period fluxes and detect potential significant effects that resulted from CO_2 injection. The network was also used as an opportunity to determine whether flux monitoring would be a practical method for environmental monitoring at commercial-scale geologic CO_2 storage projects. To evaluate the practicality of different flux monitoring methods, three installation types were tested for their relative sensitivity in measuring CO_2 fluxes.

METHODS

Soil Carbon Dioxide Flux Monitoring with the Accumulation Chamber Method

Flux Monitoring System

Soil CO_2 flux, which is the volume of CO_2 that crosses the soil surface boundary over time, was calculated as the CO_2 volume (μmol) per area (m^2) per unit of time (s) at the IBDP site. A LI-COR Biosciences LI-8100A single-chamber portable soil flux system (LI-COR Biosciences, Lincoln, Nebraska; Figure 2) was selected as a robust system for monitoring soil CO_2 fluxes at many discrete locations within the IBDP study area. The LI-8100A system uses a closed-chamber accumulation method (Madsen et al. 2009), in which air is circulated from the sealed 20-cm (7.9-in.)-diameter chamber (Figure 3) to an infrared CO_2–H_2O analyzer. Linear and exponential regressions of CO_2 concentration versus time were used to estimate initial CO_2 concentrations and calculate fluxes. Fluxes calculated by linear regression were very similar to those calculated by exponential regression. Further, a soil multiplexer was used at the site,

Table 1 Selected monitoring, verification, and accounting techniques used at the Illinois Basin – Decatur Project

Deep subsurface	Near surface
• *Geophysical surveys* to monitor CO_2 plume movement and the reservoir response to CO_2 injection • *Geochemical sampling* to monitor the responses of reservoir fluids and rock matrices to CO_2 injection and track plume movement • *Pressure and temperature monitoring* to monitor the reservoir response to CO_2 injection	• *Atmospheric monitoring* to monitor CO_2 concentrations and fluxes in the study area • *Remote sensing surveys* to determine whether land • surface movement occurred in response to CO_2 injection • *Gas surveys* to monitor soil CO_2 fluxes and soil gas concentrations • *Geochemical sampling* to evaluate whether CO_2 injection activities were affecting the shallow groundwater • *Geophysical surveys* to provide baseline conditions of earth materials within 30 m (98.4 ft) of land surface

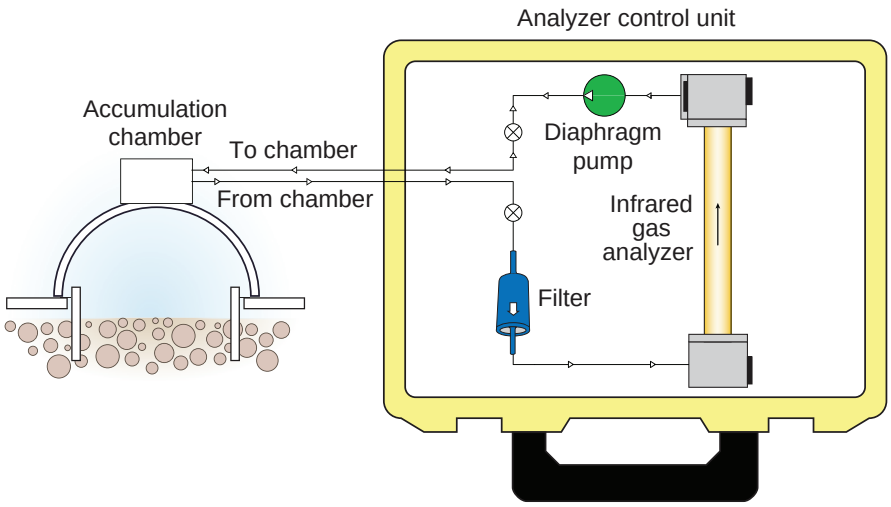

Figure 2 Schematic diagram of the LI-8100A analyzer control unit and accumulation chamber. From LI-COR Inc. (2015). Used with permission.

Figure 3 Detail of the soil CO_2 flux monitoring accumulation chamber. From LI-COR Inc. (2015). Used with permission.

and linear flux approximations from that system were intended to be directly comparable with the point flux measurements; thus, linear regression was chosen as the standard estimation of flux for the IBDP site. Concurrent soil temperature measurements were made with a rugged-penetration Type E thermocouple probe with a T handle, at approximately 10 cm (3.9 in.) below the soil surface. Concurrent soil moisture measurements were made with a ThetaProbe ML2x soil moisture sensor from Delta-T Devices (Cambridge, England). Both of these probes were connected to the LI-8100A instrument via an auxiliary sensor interface.

Polyvinylchloride (PVC) rings were inserted into the ground at each monitoring location. Rings were installed or adjusted at the beginning of each monitoring year and were periodically maintained during the field season. Each time the rings were adjusted or reset, the distance between the top of the ring and the soil surface within the new or updated ring was measured and recorded as the ring offset. The ring locations were surveyed with a handheld Trimble GPS Pathfinder Pro XR mapping-grade receiver with submeter locational accuracy (Trimble, Sunnyvale, California; Trimble 2004). Use of the set of fixed rings enabled us to collect repeated measurements at the same location systematically with no locational variability. It minimized plant and soil disturbance before flux measurements, and it provided a solid surface for the accumulation chamber to form a reliable seal (Figure 4). The accumulation chamber was seated on the ring before each measurement, removed upon completion, and moved to the next monitoring location, where the process was repeated. The rings were reset each year in response to freeze–thaw conditions, which occasionally caused them to move in the soil, altering the previously measured offsets.

Theory of Operation

Diffusion is the primary mechanism by which CO_2 moves along a gradient from high concentration to low concentration, typically from the soil to the atmosphere. However, diffusion is influenced by the CO_2 concentration gradient between the upper layers of soil and the atmosphere, which allows CO_2 to accumulate in the measurement chamber. This process can alter the gradient, potentially causing errors in flux measurements. Artificial pressure differences between the soil and the chamber, as well as rapidly increasing water vapor caused by wet soil and

Figure 4 LI-8100A analyzer control unit and accumulation chamber during field use at a bare-shallow installation.

dry atmospheric conditions, can also cause significant error in flux measurements (Welles et al. 2001). The LI-8100A system accounts for water vapor and the changing CO_2 concentration within the chamber according to the following flux calculation:

$$F_c = \left[10VP_0\left(1-\frac{W_0}{1{,}000}\right)\right] \Big/ \left[\mathrm{RS}\left(T_0+2{,}734.15\right)\left(\frac{\delta C'}{\delta t}\right)\right], \quad (1)$$

where F_c is the soil CO_2 flux (μmol $m^{-2}s^{-1}$), V is the volume (cm^3) of the system, P_0 is the initial pressure (kPa), W_0 is the initial water vapor mole fraction (mmol mol^{-1}), S is the soil surface area (cm^2), R is the gas constant (8.314 Pa m^3 mol^{-1}), T_0 is the initial air temperature (°C), and $\delta C'/\delta t$ is the initial rate of change in the water-corrected CO_2 mole fraction (μmol $mol^{-1}s^{-1}$; LI-COR Inc. 2015).

The LI-8100A system is designed to equalize pressure within the chamber to the ambient air pressure and mix the air in the chamber without requiring fans. The gasket contact between the chamber and the ring creates an effective seal that prevents atmospheric mixing and keeps the chamber from disturbing the ring (LI-COR Inc. 2015).

Experimental Design

Ring Installations

The flux monitoring network included three types of ring installations: (1) bare-shallow (Figure 5), (2) natural-shallow (Figure 6), and (3) bare-deep. Shallow rings were driven approximately 8 cm (3.1 in.) into the ground, whereas deep rings were driven approximately 46 cm (18.1 in.) into the ground. At these three types of installations, we examined the effects of (1) rings containing no vegetation, (2) rings containing natural vegetation, and (3) rings containing no vegetation that were driven deep into the soil profile to reduce the influence of root respiration on soil flux:

- The bare-shallow installation received biweekly spraying of the herbicide Roundup (Monsanto Technology LLC, St. Louis, Missouri) and biannual spraying of Pramitol 25-E (WinField Solutions LLC, St. Paul, Minnesota) in a 0.5-m (1.6-ft) radius from the center of the ring. Removal of the vegetation in and around the ring was intended to reduce the contribution of plant root respiration to flux measurements and thereby reduce the magnitude and variability of fluxes.
- The natural-shallow installation received biweekly or as-needed trimming of vegetation within the ring to keep plants from interfering with the placement of the accumulation chamber so that a representative flux measurement could be taken.

Figure 5 Bare-shallow ring installation with vegetation removed (approximately 0.5-m [1.6-ft] radius from the center of the ring).

Figure 6 Natural-shallow ring installation. Vegetation was left undisturbed if it did not interfere with the proper seating and function of the accumulation chamber.

- The bare-deep installation received the same herbicide treatment as the bare-shallow installation, but the ring was driven into the soil approximately six times deeper than the shallow-depth rings.

The bare-shallow installation type was expected to provide the greatest sensitivity to a leak signal were one to occur, so it was selected as the standard ring installation type. The three installation types were compared to verify this assumption and quantify the long-term differences among them.

The flux network area encompassed approximately 0.65 km^2 (0.25 mi^2) of land adjacent to the ADM biofuels plant (Figure 7a). A large portion of the land was previously planted in corn and soybeans. Flux monitoring locations were distributed in a grid in the field north and west of CCS1, as well as around the CCS1 injection pad. These locations were selected because of their proximity to the anticipated location of the injected CO_2 as well as to the infrastructure (i.e., the injection well) with the greatest potential for leakage. The existing infrastructure prohibited us from extending the flux monitoring network south and east of CCS1.

Ring installation began in June 2009 and was completed in September 2009. Monitoring began on June 24, 2009, and full network measurements began on September 10, 2009. The three installation types were distributed at 84 locations in groups of one, two, or three rings as follows: all 84 locations contained a bare-shallow ring installation, 30 locations included both bare-shallow and natural-shallow ring installations, and 6 locations contained all three installation types. Rings were distributed in nine rows running north to south in the main field and in two rows partially encircling CCS1 (Figure 7b). All rings were labeled with a row number and a letter (A–L) indicating the position of the ring in the row. Natural-shallow rings included an "N" label, and bare-deep rings included a "D" label (see Appendix). Installations were spaced approximately 75 m (246 ft) apart in the main field. Ring spacing near the injection well was closer: between 10 and 30 m (32.8 and 98.4 ft). Initially, the network contained 120 rings, but site activities occasionally disturbed or eliminated monitoring locations; thus, by 2015 the network had been reduced to 106 rings.

Monitoring Procedure

The LI-8100A unit and accumulation chamber were verified to be in working order each day before sampling. The equipment was inspected for damage and seal integrity, and a calibration measurement was performed to ensure the infrared gas analyzer and software were working properly. During sampling, a small utility vehicle was used to transport the soil CO_2 flux monitoring equipment between monitoring installations. Before each measurement, rings and the nearby ground were inspected for damage or disturbances that might interfere with taking a proper flux measurement. Any such discoveries were noted in the field book and used to help filter the observations during data quality assurance/quality control (QA/QC) procedures. Measurements lasted between 90 and 120 s, after which the flux data, soil temperatures, and soil moisture levels were compiled on a compact flash card during each weekly monitoring event and submitted for QA/QC review once the event was completed.

Monitoring Frequency

Fluxes were measured on a weekly basis during the growing season, typically from April to December. On days when measurements were collected, measurements were typically taken between 0700 and 1800 h. During the winter and early spring months, the frequency of flux measurements was reduced or precluded because of frozen or inundated soil conditions. Inclement weather conditions sometimes also precluded flux measurement collection. Collecting flux measurements from the entire network took between 2 and 4 days, depending on the weather.

Data Verification and Analysis

Soil CO_2 fluxes, soil temperature measurements, soil moisture measurements, meteorological data from the weather station at the Decatur Airport (5 km [3.1 mi] from the study area), and network data, including surveyed ring locations and elevations, were compiled in a Microsoft Access database developed and maintained by the Illinois State Geological Survey.

Quality Assurance/ Quality Control Criteria

A standard operating procedure was developed that incorporated the manufacturer's sampling recommendations into the IBDP flux monitoring program goals. During each measurement, soil CO_2 flux, soil temperature, and soil moisture values were monitored to ensure they were within anticipated ranges

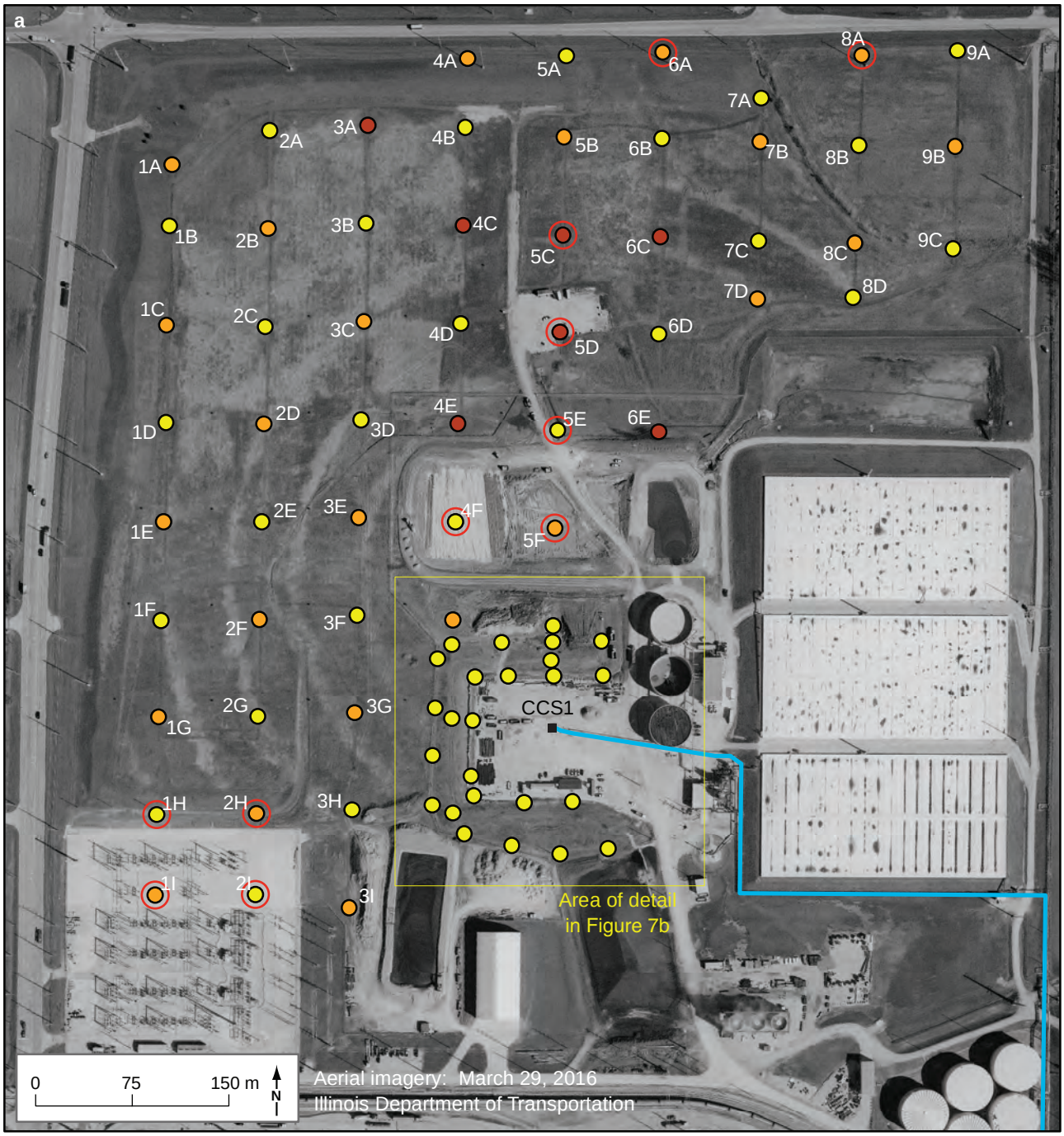

Flux ring: one treatment type

Flux ring: two treatment types

Flux ring: three treatment types

Flux ring: abandoned

CO_2 pipeline

Injection well

Figure 7 (a) The Illinois Basin – Decatur Project (IBDP) soil flux network. (b) Detail of the IBDP soil flux network area around the injection well (CCS1).

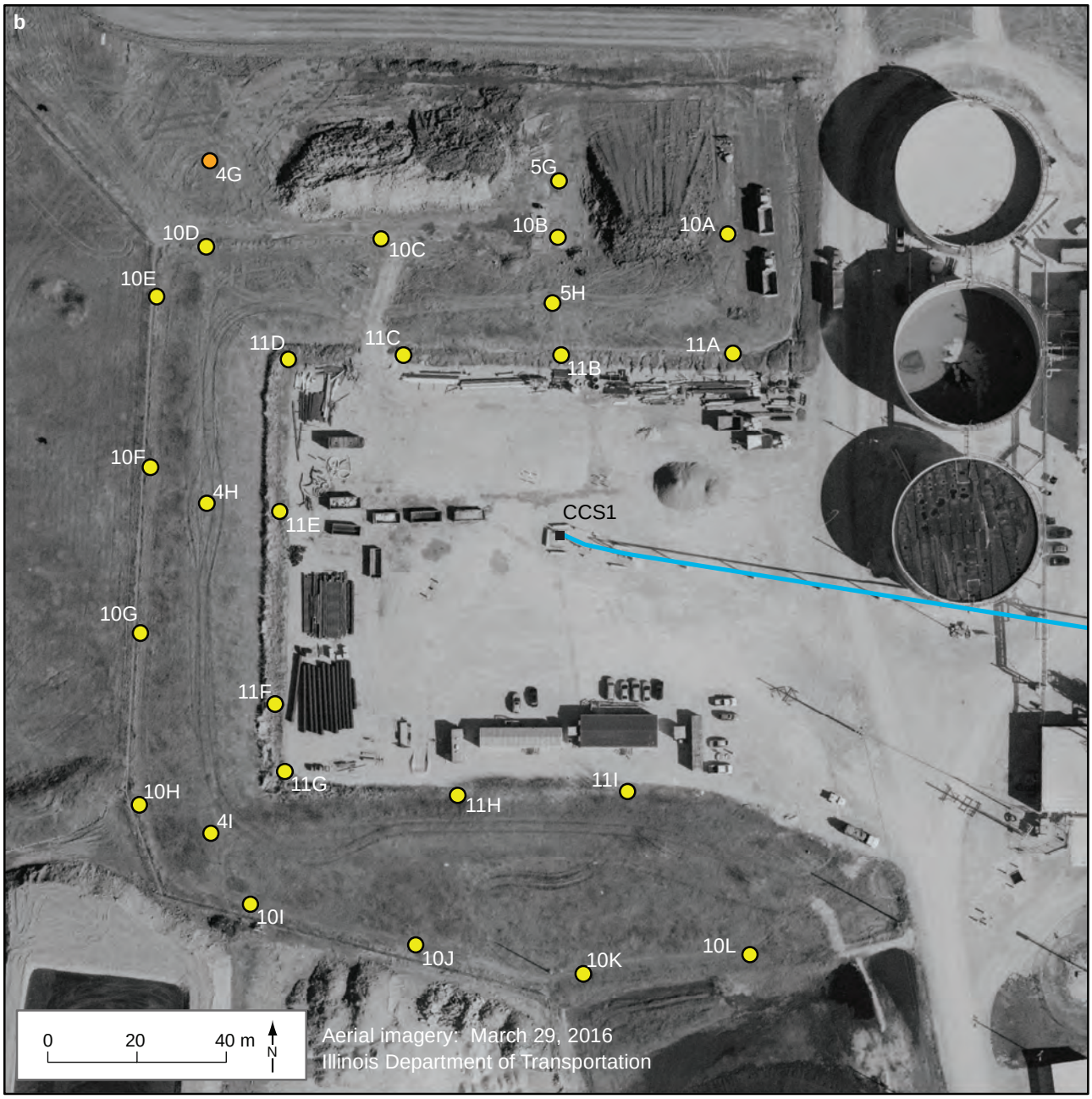

Figure 7 *Continued.*

based on current weather conditions and historical project data. Measurements that were outside the expected ranges were immediately repeated until two similar fluxes were measured consecutively. All data were retained for evaluation of the regression curves. Field notes and data were kept to detail any discrepancies in the physical condition of each monitoring location and later to verify electronic data with written records. All field data were reviewed based on a project-specific quality control review process consistent with the manufacturer's recommendations to ensure only representative data were used to calculate flux. For example, the deadband, stop time, and time-series data were reviewed for each flux estimate and modified, if required, to obtain a representative approximation of flux.

Statistical Analysis

To determine whether soil CO_2 fluxes were affected by injection-related activities, fluxes at 104 monitoring locations were divided into preinjection period and injection–postinjection period populations, separated by the beginning date of continuous, full-rate injection: November 17, 2011. A single-factor (one-way) analysis of variance (ANOVA) at an α of 0.05 was used to compare flux populations at each monitoring location. The analysis excluded data from locations 5D, 5E, 12A, 12B, and 5DN because the rings at those locations had been removed during the project to make space for additional project infrastructure and no measurements were made after injection began. For locations where the variance was found to be statistically different between the preinjection period fluxes and the injection and postinjection period fluxes, the averages of the populations were compared to determine which population had the higher average. At installations where fluxes were statistically larger during the injection and postinjection periods than the baseline fluxes, they were compared with fluxes at adjacent locations. Finally, baseline fluxes were used to establish a prediction limit (U.S. Environmental Protection Agency 2009) for the monitoring installations, and injection and postinjection period fluxes were compared with that prediction limit to identify potential flux anomalies.

Geographic Information System Analysis

Geographic information system (GIS) visualizations were used to supplement statistical data analysis and to quickly identify spatial patterns, specific monitoring locations with apparent flux abnormalities (i.e., noticeably larger or smaller fluxes relative to similar monitoring locations), or both (Korose et al. 2014). The general workflow from field monitoring to GIS analysis included verifying measurements, importing data into the project database, and using unique location identifiers to join the table of field measurement data with the table containing spatial coordinates for each measurement.

Because of the large volume of measured and derived data, the sequential and repetitive tasks of spatial data interpolation and map creation were automated by using ArcGIS software (Esri, Redlands, California). Procedures were developed to (1) select data for the time periods of interest (weeks, months, seasons, or years), (2) spatially interpolate the measured parameters by using the inverse distance weighting method (Shepard 1968), and (3) symbolize the contoured data by using a standardized classification scheme for each parameter (Korose et al. 2014). The resulting series of maps, presented as a time sequence, was a concise graphical representation of a large data set that illustrated the spatial and temporal variability of soil CO_2 fluxes and related parameters measured at the site. Weekly, monthly, seasonal, and annual maps of soil CO_2 flux, soil temperature, and soil moisture were prepared for the entire monitoring period from the summer of 2009 through the summer of 2015.

RESULTS AND DISCUSSION

Site History and Description

For several years before the IBDP site monitoring program was developed, the flux network area was irrigated with a center pivot system that used wastewater generated by ADM processing activities. The area was subsequently left fallow before and during the IBDP. Topographic relief across the network was 5.5 m (18.0 ft), from 202.0 to 207.5 m (662.7 to 680.8 ft) above sea level. The soils in the study area consisted primarily of silty loams and silty clay loams (Natural Resources Conservation Service 2014), but the original soil conditions were expected to have changed as a result of both historical land-use changes and industrial activities during the project. In some cases, soil horizons may have been completely removed or buried as a result of earthmoving that had occurred. A detailed project-specific soil survey was not conducted, so this report does not address the influence of soil type on soil CO_2 flux dynamics.

Local Weather During the Project

Air Temperature

Air temperature was evaluated to characterize its correlation with soil CO_2 flux measurements (Singh and Gupta 1977; Baldocchi et al. 2004). When soil temperature was not able to be collected consistently with each flux measurement because of equipment difficulties, air temperature was used as a proxy. The average daily air temperatures recorded at the Decatur Airport exhibited typical seasonal cycles during the flux monitoring period between 2009 and 2015 (Figure 8). Average annual temperatures for those 7 years ranged from 10.5 °C (50.9 °F) in 2014 to 13.7 °C (56.7 °F) in 2012. The warmest day was July 25, 2012 (32.0 °C, or 89.6 °F), and the coldest was January 6, 2014 (–22.2 °C, or –8.0 °F). The maximum average monthly temperature occurred in July or June, and the three warmest months in all years were June, July, and August. The minimum average monthly temperature occurred in January, February, or December, and the three coldest months in all years were December, January, and February.

Precipitation

Because soil moisture can affect fluxes (Howard and Howard 1993; Harper et al. 2005), precipitation was characterized to examine its relationship to soil CO_2 fluxes. When precipitation and soil moisture data were not able to be collected consistently on site with each flux measurement because of equipment difficulties, precipitation data from the Decatur Airport were used as a proxy. Because the Decatur Airport is 5 km (3.1 mi) from the study area, these precipitation data might not

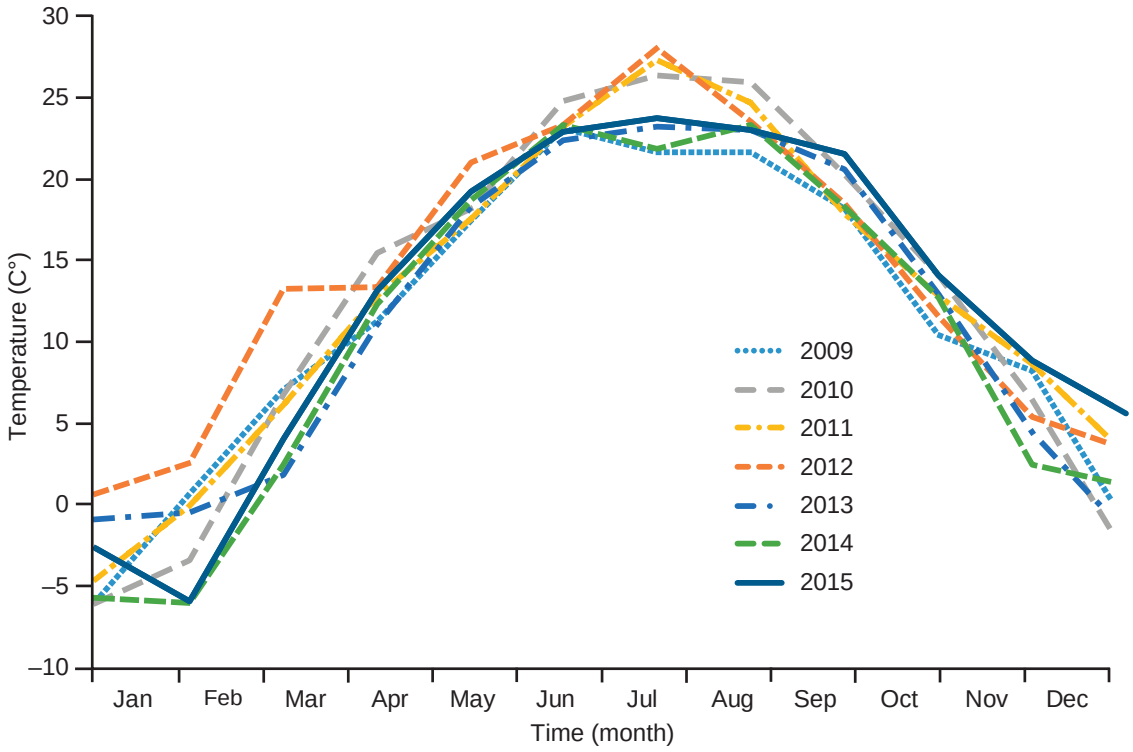

Figure 8 Average daily air temperatures (°C) recorded at the Decatur Airport during the monitoring period (2009 to 2015).

always have accurately reflected hourly or daily rainfall events at the IBDP site, although they did reflect longer term precipitation trends. The annual cumulative precipitation during the flux monitoring program ranged from 67.7 to 117.5 cm (26.7 to 46.3 in.) per year (Figure 9).

Illinois Basin – Decatur Project Soil Carbon Dioxide Fluxes

Three installation types were used to evaluate the relative effectiveness of each type in detecting leakage. Fluxes ranged from –0.5 to 76.3 μmol $m^{-2}s^{-1}$ at the bare-shallow installations, from 0.1 to 25.6 μmol $m^{-2}s^{-1}$ at the natural-shallow installations, and from 0.1 to 9.7 μmol $m^{-2}s^{-1}$ at the bare-deep installations (Table 2). The average fluxes throughout all 7 years were 1.9 ± 2.2 μmol $m^{-2}s^{-1}$ (bare-shallow), 5.1 ± 3.8 μmol $m^{-2}s^{-1}$ (natural-shallow), and 1.7 ± 1.6 μmol $m^{-2}s^{-1}$ (bare-deep). Fluxes measured at natural-shallow monitoring locations throughout the entire monitoring period were 2.7 times larger than those measured at bare-shallow monitoring locations (Table 2). In general, fluxes at the natural soil installations were greater than those at the bare soil installations, and fluxes were slightly larger at the bare-shallow installations than at the bare-deep installations.

Soil CO_2 flux consists of the cumulative aerobic respiration of plant roots, fungi, animals, and bacteria, combined with CO_2 produced by the decomposition of surface litter and soil organic matter (Singh and Gupta 1977) and any anthropogenically introduced CO_2. The respiration processes are primarily influenced by soil temperature changes and occasionally by acute soil moisture changes (Howard and Howard 1993; Raich and Potter 1995). Consequently, flux patterns are related to diurnal and seasonal temperature changes and precipitation patterns caused by the local climate (Edwards and Harris 1977; Fang and Moncrieff 2001).

Temperature

Soil CO_2 fluxes were generally greatest in the soil temperature range of 10 to 30 °C (50 to 86 °F) for all three installation types (Figure 10). Fluxes were smallest and most narrowly distributed at soil temperatures near 0 °C (0 °F), whereas fluxes increased and the range of fluxes became greater as the soil temperature increased. The response of flux to temperature was proportionally consistent across the installation types, despite the generally larger magnitude of fluxes at the natural-shallow locations.

Drought Impact

In 2012, a drought affected the soil CO_2 fluxes measured at the IBDP site. Cumulative precipitation in 2012 was only 67.7 cm (26.7 in.), or 29% below the site average of 95.4 cm (37.6 in.) from 2009 to 2015. The drought occurred from April through July 2012, during which cumulative precipitation was 16.0 cm (6.3 in.), 64% below the site average of 43.9 cm (17.3 in.) from April through July for all other years. Precipitation is essential for plant growth and respiration during the early portion of the growing season, which is typically April through June in the U.S. Midwest. It is therefore understandable that bare-shallow fluxes were significantly smaller in 2012 (Figure 11) than in other years. Soil CO_2 fluxes were 37% lower than the site average for April through July.

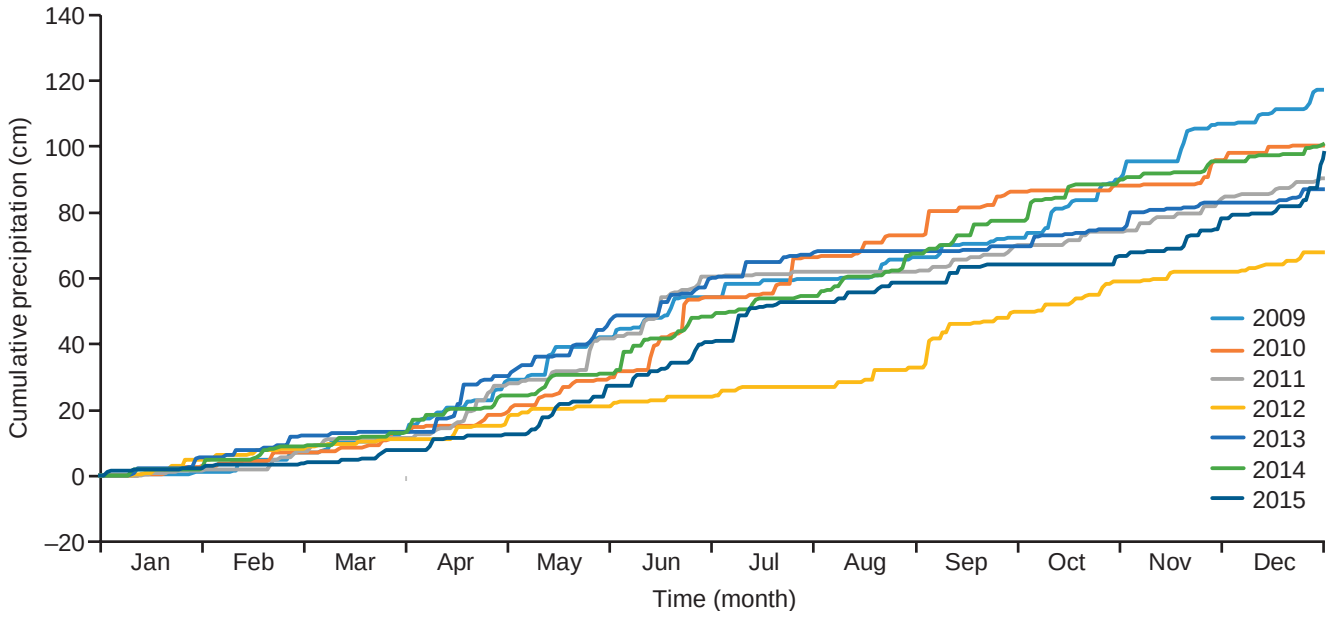

Figure 9 Annual cumulative daily precipitation (cm) recorded at the Decatur Airport during the monitoring period (2009 to 2015).

Table 2 Summary of flux measurements at the Illinois Basin – Decatur Project from 2009 to 2015[1]

Year	Installation type	Number of flux measurements	Minimum	Average	Maximum	Standard deviation
2009	Bare-shallow	1,014	0.1	2.1	27.6	1.9
	Natural-shallow	226	0.1	3.0	15.4	2.8
	Bare-deep	30	0.2	3.4	9.7	3.1
2010	Bare-shallow	1,209	0.1	2.3	20.9	2.0
	Natural-shallow	480	0.2	5.5	25.6	4.2
	Bare-deep	72	0.2	1.8	7.4	1.3
2011	Bare-shallow	1,191	0.1	2.1	76.3	3.9
	Natural-shallow	574	0.2	4.0	16.9	3.4
	Bare-deep	72	0.2	1.6	7.8	1.4
2012	Bare-shallow	2,398	0.1	1.5	23.8	1.6
	Natural-shallow	916	0.2	4.4	21.3	2.8
	Bare-deep	154	0.1	1.5	7.0	1.2
2013	Bare-shallow	2,037	0.1	1.7	17.6	1.8
	Natural-shallow	767	0.2	5.1	20.5	3.6
	Bare-deep	112	0.1	1.4	8.7	1.4
2014	Bare-shallow	1,023	0.1	2.3	11.0	1.7
	Natural-shallow	340	0.5	8.7	25.3	4.8
	Bare-deep	35	0.2	2.2	8.6	1.5
2015	Bare-shallow	181	–0.5	2.9	13.9	3.0
	Natural-shallow	73	2.3	8.7	22.8	4.0
	Bare-deep[2]	—	—	—	—	—
All years	Bare-shallow	9,053	–0.5	1.9	76.3	2.2
	Natural-shallow	3,376	0.1	5.1	25.6	3.8
	Bare-deep	475	0.1	1.7	9.7	1.6

[1]Minimum, average, maximum, and standard deviation values are given in micromoles per square meter per second (μmol $m^{-2}s^{-1}$).
[2]No measurements were collected at bare-deep rings in 2015 because the rings generally contained rainwater or the soil within the ring was completely saturated because of poor drainage during the period when flux measurements were taken.

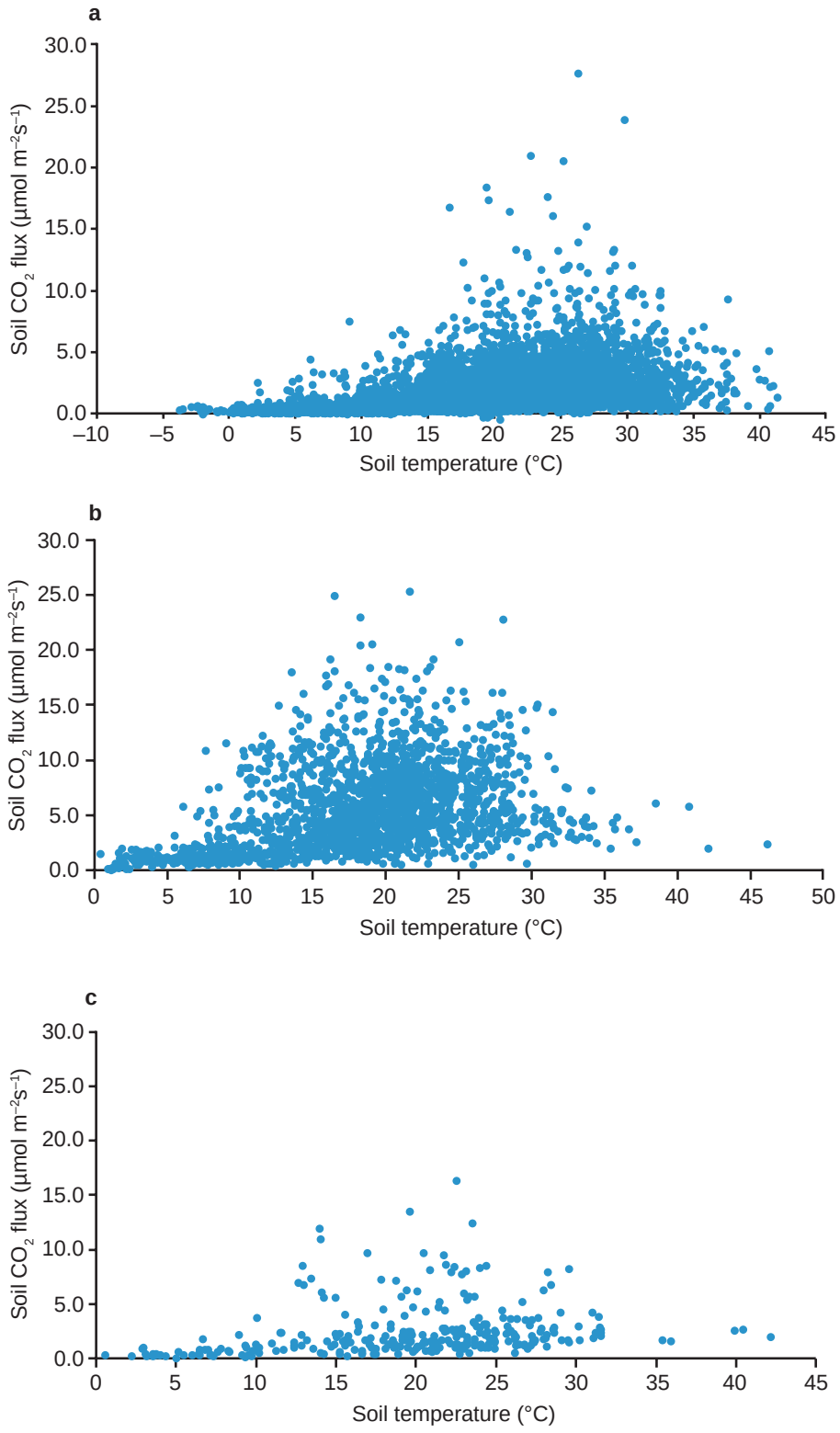

Figure 10 Distribution of soil CO_2 flux values in relation to soil temperature for the (a) bare-shallow, (b) natural-shallow, and (c) bare-deep installations. (d) Average fluxes for 5 °C (41 °F) soil temperature intervals. (*Continued on next page.*)

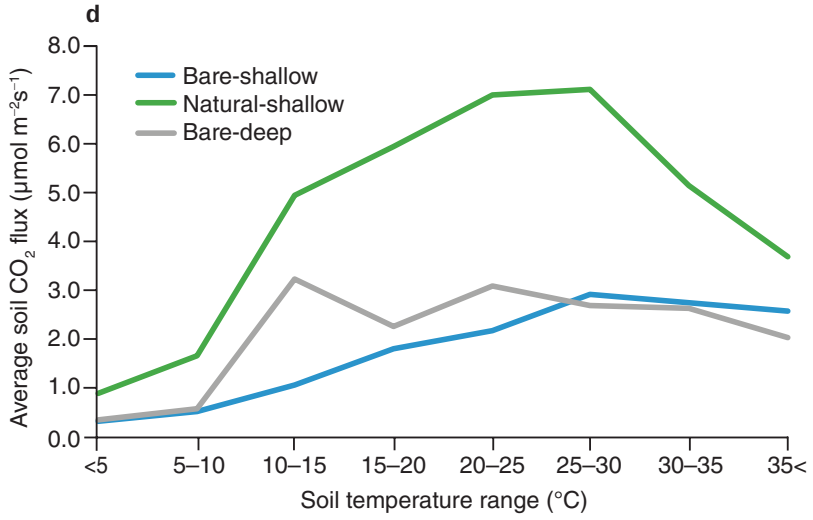

Figure 10 *Continued.*

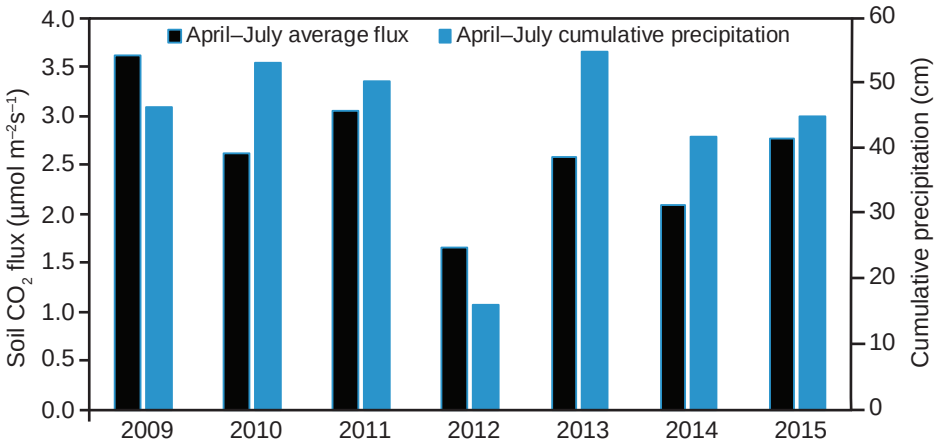

Figure 11 Average monthly bare-shallow soil CO_2 flux and cumulative precipitation for April through July of each monitoring year.

Seasonality

The seasons were defined as follows: (1) spring included March, April, and May; (2) summer included June, July, and August; (3) fall included September, October, and November; and (4) winter included December, January, and February. Soil CO_2 fluxes followed the same general seasonal trend during each year of monitoring: fluxes were largest in the summer and smallest in the winter at both the bare-shallow and natural-shallow installations (Carman et al. 2014; Table 3 and Figure 12). Freezing temperatures often prohibited the collection of flux measurements, so monitoring was performed during the winter season only in 2009, 2011, and 2013 (Figure 12) as the weather allowed. The limited ability to collect flux measurements during the winter season is considered a significant drawback of this specific monitoring technique.

Soil temperatures measured at the bare-shallow and natural-shallow installations followed the same seasonal pattern as soil CO_2 fluxes and were also closely related to the air temperature (Figure 12a–g) measured at the Decatur Airport. Soil temperatures (Figure 12a–g) were generally higher than air temperatures because the air temperature was a daily average whereas soil temperatures were measured only during monitoring, typically between 0700 and 1800 h.

Effects of Installation Type on Soil Carbon Dioxide Fluxes

Comparison of Installation Types

As described in the Methods section (see Soil Carbon Dioxide Flux Monitoring with the Accumulation Chamber Method on p. 2), three installation types were tested within the IBDP flux monitoring network: (1) bare-shallow, (2) natural-shallow, and (3) bare-deep. To facilitate data comparison and interpretation, the natural-shallow rings were paired with the bare-shallow rings. Similarly, the bare-deep rings were grouped with both bare-shallow and natural-shallow rings. All three installation types were collocated at five locations in the study area:

Table 3 Average soil CO_2 fluxes by season and installation type across all monitoring years

	Bare-shallow		Natural-shallow	
Season	Average flux	Standard deviation	Average flux	Standard deviation
Spring	1.5	0.6	4.9	1.5
Summer	2.5	0.9	6.9	1.4
Fall	1.1	1.1	2.8	0.7
Winter	0.2	0.1	0.7	0.3

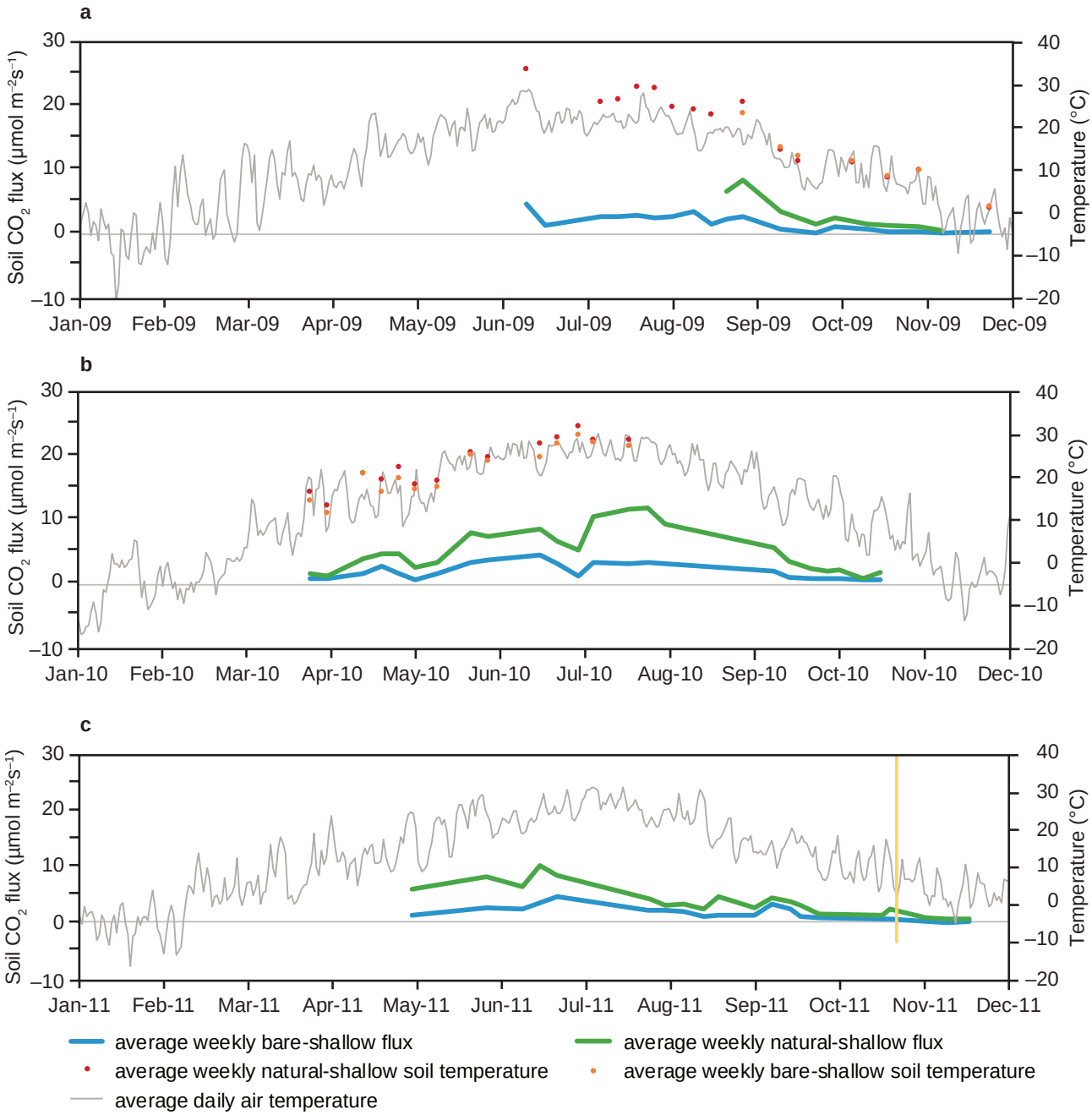

Figure 12 Average weekly bare-shallow (blue lines) and natural-shallow (green lines) fluxes, average daily air temperature (°C) as measured at the Decatur Airport (gray lines), and average weekly soil temperature at the bare-shallow (red circles) and natural-shallow (orange circles) installations: (a) 2009, (b) 2010, (c) 2011, (d) 2012, (e) 2013, (f) 2014, and (g) 2015. The beginning of injection is represented by a yellow line (c), and the end of injection is represented by a purple line (f). (*Continued on next page.*)

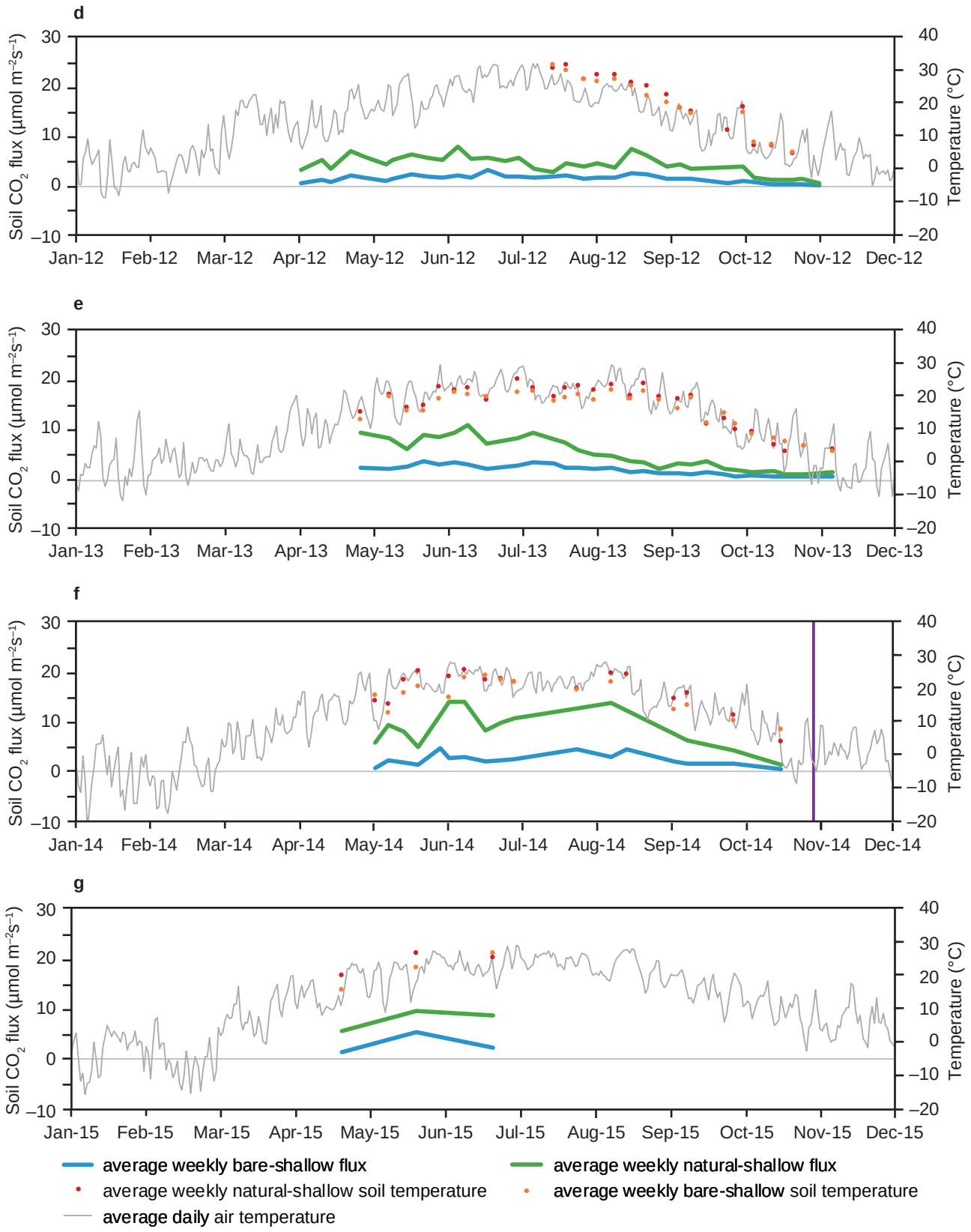

Figure 12 *Continued.*

Table 4 Average soil CO_2 flux and standard deviation by installation type at five monitoring locations that contained all three soil installation types

	Average soil CO_2 flux (μmol $m^{-2}s^{-1}$ ± standard deviation)		
Monitoring location	Bare-shallow	Natural-shallow	Bare-deep
3A	1.5 ± 1.1 (*n* = 138)	4.9 ± 3.6 (*n* = 125)	1.8 ± 1.2 (*n* = 122)
4C	1.6 ± 1.6 (*n* = 122)	5.3 ± 3.6 (*n* = 123)	1.8 ± 1.7 (*n* = 80)
4E	1.3 ± 1.0 (*n* = 113)	4.2 ± 3.7 (*n* = 116)	1.4 ± 1.5 (*n* = 97)
6C	1.6 ± 1.1 (*n* = 119)	4.8 ± 4.0 (*n* = 117)	1.6 ± 1.9 (*n* = 73)
6E	1.8 ± 1.3 (*n* = 108)	4.6 ± 3.7 (*n* = 117)	1.6 ± 1.6 (*n* = 96)

3A, 4C, 4E, 6C, and 6E (see Figure 7). Among these five locations, the average soil CO_2 flux measured over the course of the project (from June 24, 2009, to July 9, 2015) at natural-shallow locations was between 4.2 ± 3.7 (4E) and 5.3 ± 3.6 μmol $m^{-2}s^{-1}$ (4C). The average flux was between 1.3 ± 1.0 (4E) and 1.8 ± 1.3 μmol $m^{-2}s^{-1}$ (6E) at bare-shallow installations, and it was between 1.4 ± 1.5 (4E) and 1.8 ± 1.7 μmol $m^{-2}s^{-1}$ (4C) at bare-deep installations (Table 4).

Soil CO_2 flux is primarily driven by the presence of organic matter and plant root respiration, and vegetation was eliminated at the bare soil installations. Thus, the average and standard deviation of soil CO_2 fluxes measured at the bare soil installations were approximately three times smaller than those of fluxes measured at the natural soil installations. As anticipated, fluxes measured at the bare soil installations were smaller and less variable; therefore, on the basis of these results, the bare-shallow type is suggested as the preferred installation type because it is the most sensitive to the detection of anomalous fluxes resulting from a surface CO_2 leak.

Practical Considerations

The time required for installation maintenance was different for the bare and natural installation types. Application of herbicide at the combined 79 bare-shallow and bare-deep installations required approximately 8 min per ring to complete, whereas trimming at the natural-shallow installations required approximately 4 min per ring to complete (as estimated from the total time required for each maintenance activity and the total number of rings maintained).

Three soil installation types were used during the project. Rings for the bare-deep installation type did not drain water as well as rings at the shallow-deep installations because of their greater insertion depth into the soil. The inability to drain quickly meant the rings frequently contained standing water, which precluded collection of soil CO_2 flux measurements. For example, at monitoring locations 4C and 4D (Figure 7a), the rings contained standing water during all of 2014, and no measurements were able to be made at those locations. Because of consistently poor drainage of the bare-deep rings in 2015, flux measurements were made only at the bare-shallow and natural-shallow monitoring locations.

Analysis of Preinjection Period Versus Injection Period and Postinjection Period Fluxes

If a leak were to occur, it was expected to present as large localized fluxes limited to relatively small areas, in patches up to 20 m (65.6 ft) in diameter (Lewicki et al. 2009; Feitz et al. 2014). Therefore, our statistical analysis focused on comparing preinjection period fluxes with injection and postinjection period fluxes at individual rings. We used GIS mapping of average fluxes over various time periods (weeks, months, seasons, and years) to investigate the possibility of sustained increased fluxes over a greater area (see ArcGIS Flux Maps section below).

Statistical Results and Interpretation

Preinjection period fluxes were compared with injection and postinjection period fluxes with a single-factor (one-way) ANOVA, at an α of 0.05, at 104 of the 109 monitoring locations (no measurements were made at locations 5D, 5E, 12A, 12B, and 5DN after injection began). Two bare-shallow (2B and 4H; Figure 7a,b) and four natural-shallow (1AN, 1CN, 1EN, and 1IN) installations were found to have significantly different fluxes between the preinjection period and the injection and postinjection periods and had a greater average flux after injection began. Rings 2B, 1AN, 1CN, 1EN, and 1IN were collocated within 2 m (6.6 ft) of rings 2BN, 1A, 1C, 1E, and 1I, respectively. The ANOVA indicated no significant difference between preinjection period fluxes and injection and postinjection period fluxes at any of those five collocated rings (Figure 13). Ring 4H (Figure 14) was part of a higher density portion of the monitoring network surrounding CCS1, where rings were installed between 10 and 30 m (32.8 and 98.4 ft) of each other (Figure 7b). The ANOVA results indicated that fluxes measured at all other 23 monitoring locations near CCS1 were not significantly larger during injection and postinjection than during preinjection. Anomalous fluxes, defined as those that exceeded the prediction limit calculated from baseline data, occurred at four of the six rings. No anomalous fluxes were detected with the prediction limit test at ring 1CN or ring 1IN. In addition, anomalies were both infrequent and inconsistent: all the anomalous soil CO_2 fluxes at 2B, 4H, 1AN, and 1EN occurred intermittently between April 30 and September 24, during the height of the local growing season. Therefore, the change in flux between preinjection and injection or postinjection at these locations indicated false positives caused by the general variability and larger relative magnitude of fluxes during the growing season.

ArcGIS Flux Maps

ArcGIS was used to generate maps with spatial interpolation from weekly, monthly, seasonal, or yearly flux averages from each bare-shallow and natural-shallow monitoring installation. Because of the relative difference in flux magnitudes

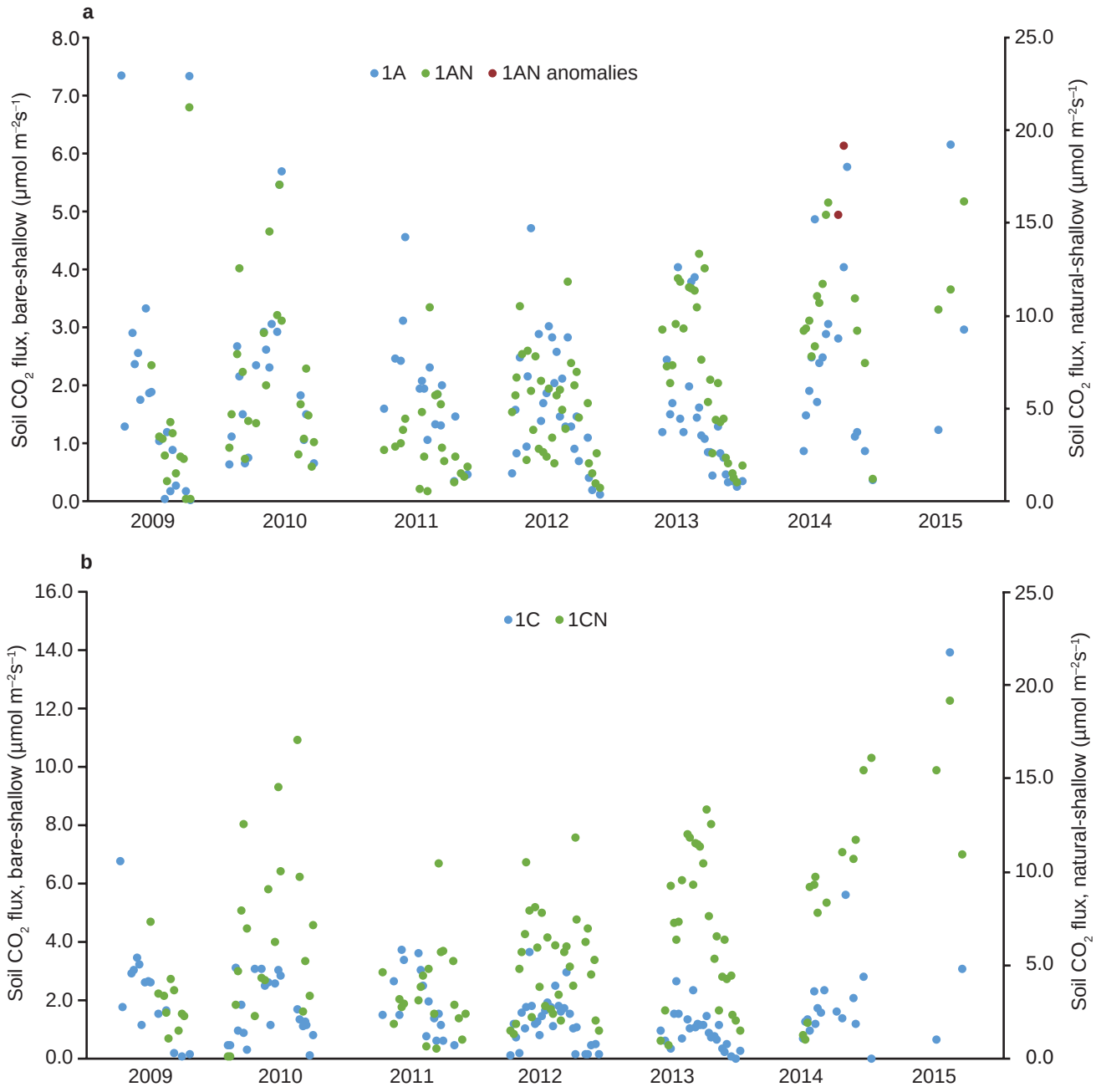

Figure 13 (a–e) Anomalous fluxes at natural-shallow installations compared with typical fluxes and fluxes measured at adjacent bare-shallow installations. Anomalous fluxes are shown in red. (d) These two installations (1I, 1IN) were removed in the middle of the 2013 monitoring campaign to make way for the expanding infrastructure. (*Continued on next page.*)

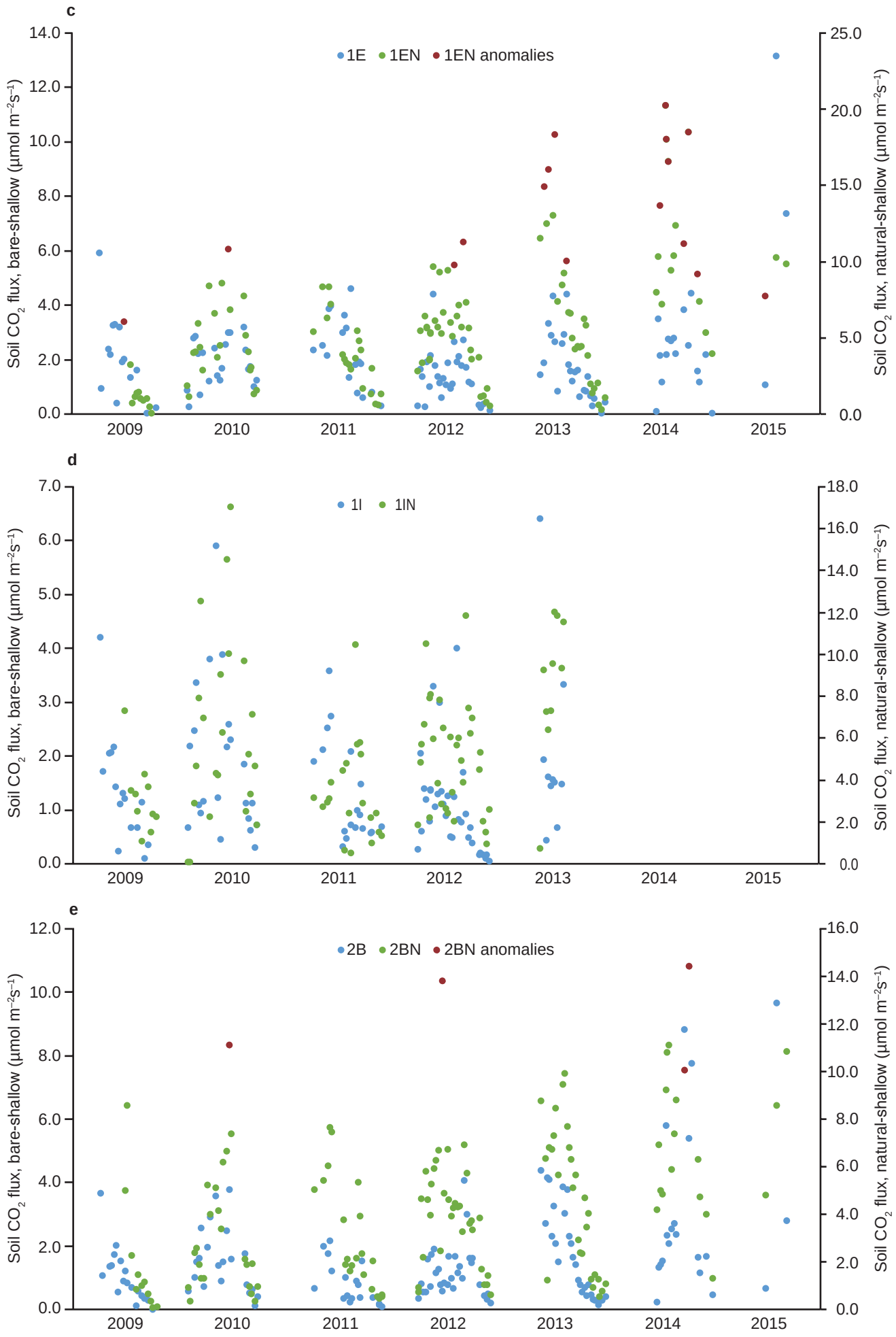

Figure 13 *Continued.*

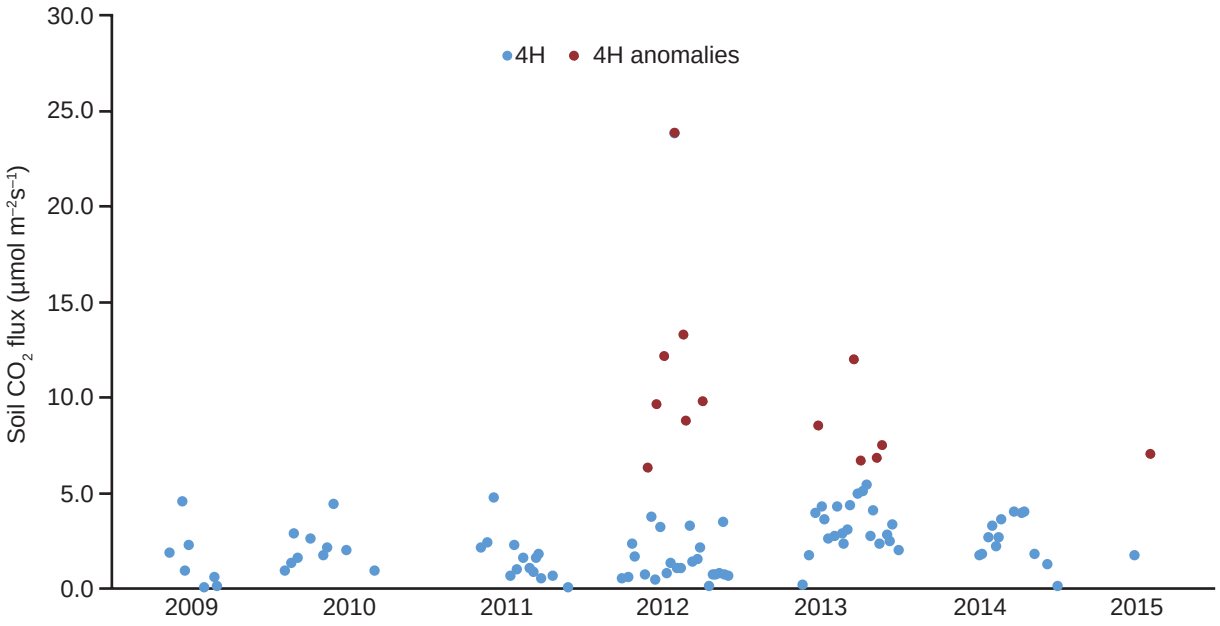

Figure 14 Soil CO_2 fluxes at monitoring location 4H, a bare-shallow installation. Fluxes identified as anomalous are shown in red.

for the bare versus natural rings, different color schemes were chosen to best display and explore each data set. It should be noted that varying numbers of monitoring events were used to produce the monthly ($1 \le n \le 5$), seasonal ($1 \le n \le 13$), and yearly ($3 \le n \le 32$) flux maps. Because of the variability of flux values observed, changes in the number of monitoring events used for the averages may have produced biases in the maps by allowing incomplete or inaccurate representation of the actual fluxes during a specific time period.

For example, the monthly map produced from bare-shallow fluxes for June of 2015 indicates that fluxes were comparatively large during that period (Figure 15). However, our statistical analysis determined that only one flux during that monitoring event was potentially anomalous (at installation 4H on June 4, 2015) and it was subsequently determined to be unrelated to CO_2 injection (Figure14). Because the rest of the fluxes used to generate the map were within baseline variability, the large fluxes observed on the map were likely due to the smaller sample size used to generate the monthly average.

Statistical and graphical analyses of fluxes were supplemented with flux maps to help identify significant flux anomalies and variations that might have indicated leakage. Statistical flux anomalies were identified, reviewed, and systematically evaluated, and all anomalies were ultimately attributed to factors unrelated to CO_2 injection. Maps of monthly flux averages (Figure 15) were used to identify two instances in which relatively larger fluxes occurred at individual rings: three consecutive large fluxes were observed in 2011 at location 5H, and an extended period of larger fluxes was observed at location 11I in the spring and summer of 2013 (Figure 7b). The larger fluxes observed at 5H all occurred before CO_2 injection at CCS1 and therefore could not have been the surface expression of injection leakage. During 2013, fluxes measured at location 11I were 3.6 and 3.3 times greater in the spring and summer, respectively, than the site average of bare-shallow flux measurements. A review of field notes showed that this monitoring location was inaccessible to spraying equipment until fall because of wet field conditions. Thus, in spring and summer, vegetation grew inside and around the ring and contributed to larger soil CO_2 fluxes for that time period. In other words, the monitoring protocol could not be followed at that location, which resulted in anomalously large measurements. Fluxes returned to the expected range once normal ring maintenance resumed.

Seasonality

Despite the seasonal variability apparent in the monthly flux maps for both the bare and natural rings, the maps of flux magnitudes exhibited no spatial patterns that would suggest leakage of the injected CO_2. Fluxes were related to the growing season, each year peaking in late summer or early fall and then decreasing to about zero by late fall or early winter.

SUMMARY

Analysis of Fluxes for Leak Detection

Baseline preinjection period soil CO_2 fluxes were compared by ANOVA with injection and postinjection period fluxes at each monitoring location and installation type. The results indicated that the fluxes that occurred after injection began were significantly larger than the baseline fluxes at six monitoring installations: two bare-shallow locations (2B and 4H) and four natural-shallow locations (1AN, 1CN, 1EN, and 1IN). Locations 2B, 1AN, 1CN, 1EN, and 1IN were collocated within 2 m (6.6 ft) of monitoring locations 2BN, 1A, 1C, 1E, and 1I, respectively (see Appendix). The ANOVA results indicated that fluxes at all five of those collocated installations showed no significant increase between the preinjection period

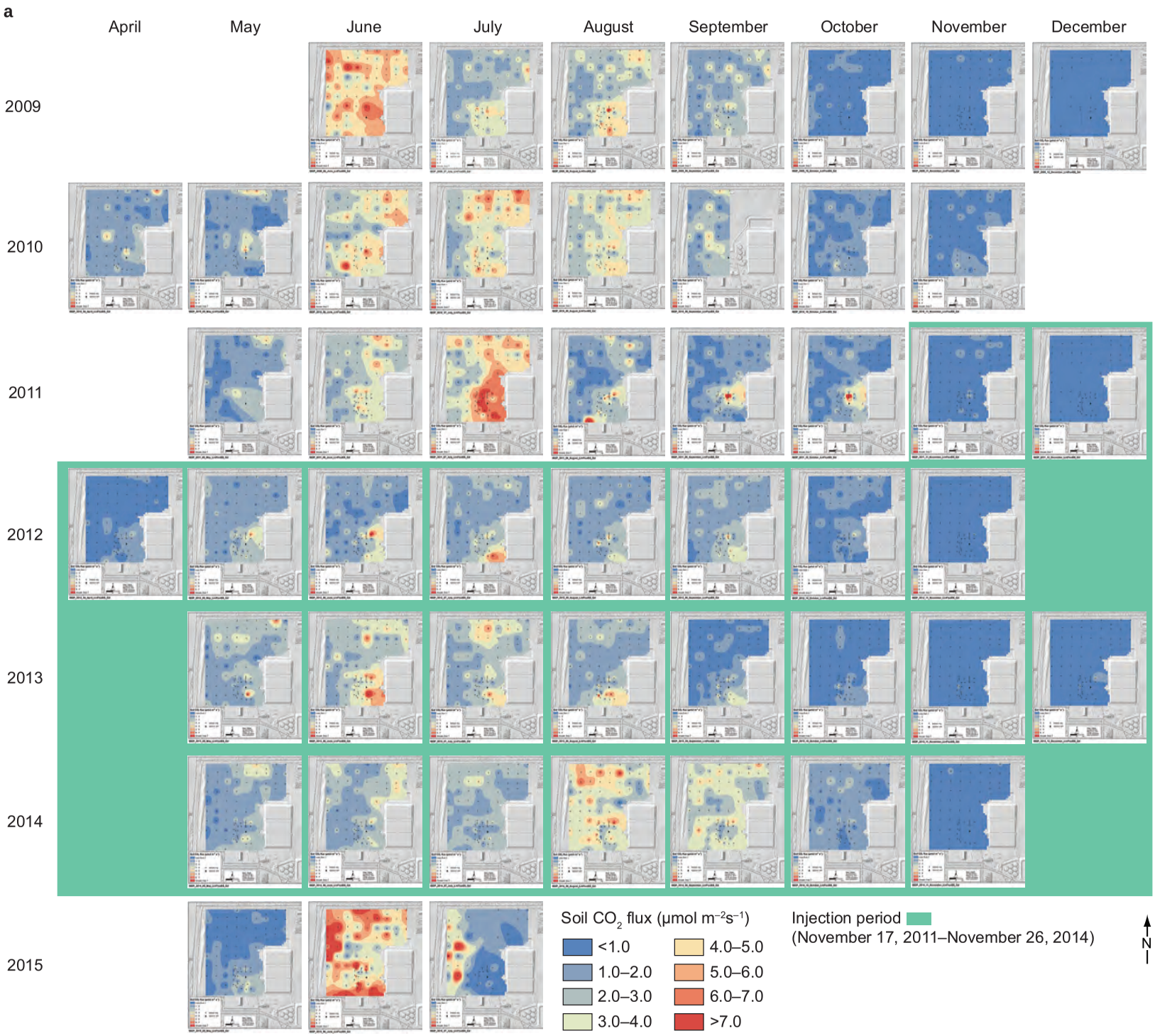

Figure 15 Monthly average flux maps created in ArcGIS from fluxes measured at (a) bare-shallow and (b) natural-shallow installation types. (*Continued on next page.*)

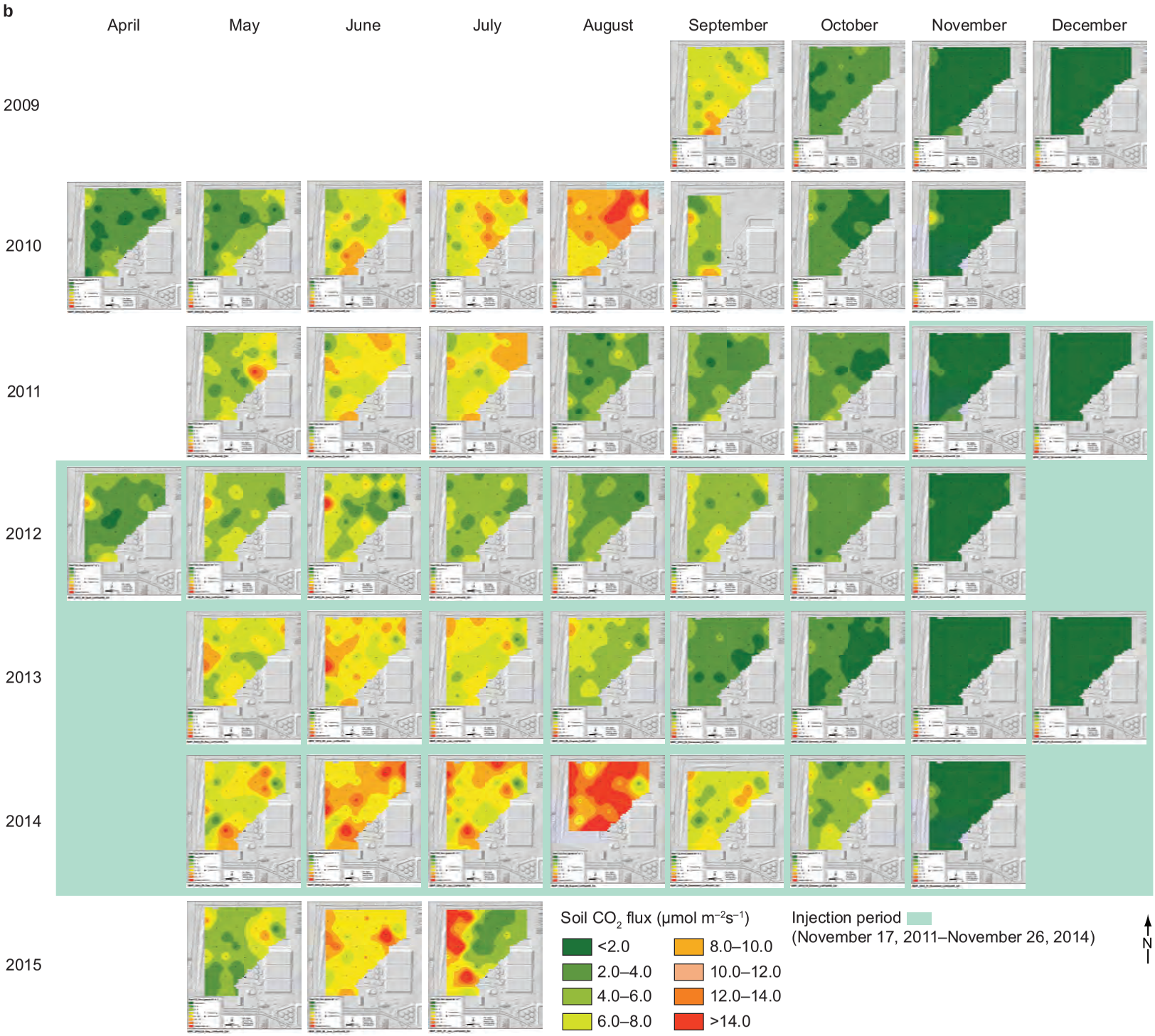

Figure 15 *Continued.*

and the injection or postinjection period. Although no rings were directly collocated with monitoring location 4H, it was part of a denser field of monitoring locations surrounding CCS1, where rings were installed between 10 and 30 m (32.8 and 98.4 ft) apart from each other (Figure 7b). The ANOVA results indicated that none of the 23 other flux monitoring installations in that higher density portion of the monitoring network showed significant increases in flux between the preinjection period and the injection and postinjection periods. Fluxes identified as anomalous occurred infrequently and inconsistently at all six of these installations during the growing season only. Therefore, the atypical fluxes at 2B, 4H, 1AN, 1CN, 1EN, and 2BN were attributed to the generally high variability and large magnitude of fluxes during the growing season (see Appendix).

Illinois Basin – Decatur Project Climate and Flux Trends

Air temperature measured at the Decatur Airport followed similar seasonal trends. In each monitoring year, as expected, the warmest 3 months were June, July, and August (summer season), and the coldest 3 months were December, January, and February (winter season). The magnitude of soil CO_2 flux at the IBDP was well correlated with soil temperature throughout monitoring, and it showed impacts from very low or very high soil moisture values. The impact of soil moisture on fluxes was most evident during extremely dry periods, such as the late spring and summer drought of 2012.

Installation Types

Three installation types, (1) bare-shallow, (2) natural-shallow, and (3) bare-deep installations, were tested at the IBDP to quantify how the presence or absence of vegetation and the insertion depth of the rings affected soil fluxes. Overall, herbicide treatment in and around the rings reduced the magnitude and variability of fluxes. The soil CO_2 fluxes measured at both the bare-shallow and bare-deep installations were similar, but vegetation at the natural-shallow installations increased fluxes by approximately 2.7 times over those measured at the collocated bare-shallow installations.

Recommendations

Soil Carbon Dioxide Flux Monitoring

Because of the significant research focus of the flux monitoring program at the IBDP, it was more time and resource intensive than would be economical at a commercial-scale CCS project. Further, soil flux monitoring may be a relatively inefficient method of leakage detection because CO_2 leaks are anticipated to have limited surface expression. However, soil CO_2 flux monitoring could be used to determine the natural variability and characterization of fluxes to quantify soil flux rates as part of a leakage assessment if a leak were suspected or known to have occurred. When considering a soil flux monitoring program at long-term or commercial-scale CCS projects, site-specific risks, costs, and benefits should be evaluated and soil flux monitoring should be used based on site-specific needs.

Baseline and Supplementary Flux Data

Soil CO_2 fluxes at the IBDP exhibited natural variability and seasonality related to the local growing season, temperature, and extremes in soil moisture. Therefore, to accurately determine whether injection activities at a CCS site have affected soil fluxes, enough baseline data are necessary to establish the range of natural variability. For the IBDP, a monitoring period of multiple years was required to observe minima and maxima of soil and weather conditions. In addition to soil CO_2 flux measurements, supplementary soil temperature and soil moisture data were useful in determining the site-specific response of fluxes to various soil conditions. Detailed records of site activities were also shown to be important in determining the provenance of fluxes that appeared anomalous.

Monitoring Method

Soil fluxes were lowest during the winter months, so a leakage signal caused by a persistent leak should be the most easily detected during that season. However, flux measurements with the accumulation chamber method were often prevented by rain during the spring and summer and by snow in the winter months. Therefore, if the accumulation chamber method is used to measure fluxes during the growing season, alternative systems could be used for wintertime monitoring. Closed-chamber or eddy covariance monitoring may be alternative methods for continuing flux monitoring during the winter (Janssens et al. 2000).

Installation Type Recommendations

At the IBDP, the bare-shallow and natural-shallow installation types provided different benefits. Generally, we recommend the bare-shallow installation as the preferred type for monitoring soil CO_2 flux at an industrial CCS site. Fluxes at the bare-shallow type were smaller and less variable than those at the natural-shallow type and therefore should more effectively identify smaller changes in soil flux that could be related to a leak. However, the bare-shallow installation required several weeks before the herbicide eliminated vegetation within the desired radius from the center of the ring. In contrast, the natural-shallow installations required less maintenance and development time than did the bare-shallow installations, which could reduce the cost of monitoring soil CO_2 fluxes at commercial-scale CCS projects but would result in greater variability in flux measurements and less sensitivity for the purpose of leak detection. We do not recommend using the bare-deep installation type for leak detection in a soil CO_2 flux monitoring network at a CCS project: poor drainage of the rings led to frequent inundation, which often precluded flux measurement collection. Soil CO_2 flux monitoring is farther removed from the reservoir and is therefore likely to detect leakage signatures later than other higher priority monitoring techniques such as deep fluid monitoring and geophysical monitoring.

Monitoring Plan Recommendations

A commercial-scale CCS project using the soil flux monitoring technique would perhaps use a much less resource-intensive soil CO_2 flux monitoring program than was used at the IBDP. In addition, the purchase of a soil flux monitoring system solely for project use represents a significant financial investment in terms of both the initial equipment purchase and the annual maintenance and recalibration costs.

We also recommend less frequent monitoring than was performed at the IBDP. Flux measurements should be made during each season at all monitoring

Table 5 Description of data available for download on request

Statistic	Units	Description
Label	NA	Assigned name of the monitoring installation at which the flux measurement was made
DateTime	MM/DD/YYYY HH:MM	Date and time at the beginning of the flux measurement
Flux	μmol $m^{-2}s^{-1}$	Value of the flux, calculated by linear regression of the CO_2 concentration over time
R^2	NA	Coefficient of determination of the flux regression curve
SoilTemp	°C	Average soil temperature recorded during the associated flux measurement
ChamberTemp	°C	Average temperature within the chamber recorded during the flux measurement
IV_H_2O	$mmol_{H2O}/mol_{air}$	Initial water vapor concentration value
IV_CO_2	$\mu mol_{CO2}/mol_{air}$	Initial CO_2 concentration value
IV_C_{dry}	$\mu mol_{CO2}/mol_{air}$	Initial CO_2 concentration value after correction for water vapor dilution

installations to accurately capture seasonal variability and establish baseline ranges for fluxes at a project site. Subsequent monitoring during the injection and postinjection periods should be defined by the baseline frequency and the observed variability of fluxes during baseline monitoring.

Accompanying Digital Data

For researchers who wish to conduct further analyses, soil CO_2 flux data collected at the IBDP from 2009 to 2015 are available on request in electronic format. Nine parameters or results are available for each flux measurement (Table 5). To request data, contact the Illinois State Geological Survey at https://isgs.illinois.edu/data-help-request.

ACKNOWLEDGMENTS

The Midwest Geological Sequestration Consortium is funded by the U.S. Department of Energy through the National Energy Technology Laboratory via the Regional Carbon Sequestration Partnership Program (contract number DE-FC26-05NT42588) and by a cost share agreement with the Illinois Department of Commerce and Economic Opportunity, Office of Coal Development. The authors thank the following individuals for their contributions to the development of this report: Damon Garner assisted with database development and Abbas Iranmanesh with statistical analysis; Elizabeth Curtis-Robinson, Nicholas Chin, Jacquelyn Hurry, and Christopher Patterson helped collect weekly flux data; and William Bruns assisted with the installation and maintenance of the network. The authors also thank the ISGS review team, and especially Ivan Krapac for his invaluable insights and assistance to the project throughout.

REFERENCES

Baldocchi, D.D, L. Xu, and N. Kiang, 2004, How plant functional-type, weather, seasonal drought, and soil physical properties alter water and energy fluxes of an oak-grass savanna and an annual grassland: Agricultural and Forest Meteorology, v. 123, no. 1–2, p. 13–39, https://doi.org/10.1016/j.agrformet.2003.11.006.

Carman, C.H., R.A. Locke II, and C.S. Blakley, 2014, Update on soil CO_2 flux monitoring at the Illinois Basin – Decatur Project, USA: Energy Procedia, v. 63, p. 3869–3880, https://doi.org/10.1016/j.egypro.2014.11.417.

Edwards, N.T., and W.F. Harris, 1977, Carbon cycling in a mixed deciduous forest floor: Ecology, v. 58, no. 2, p. 431–437, https://doi.org/10.2307/1935618.

Fang, C., and J.B. Moncrieff, 2001, The dependence of soil CO_2 efflux on temperature: Soil Biology and Biochemistry, v. 33, no. 2, p. 155–165, https://doi.org/10.1016/S0038-0717(00)00125-5.

Feitz, A., C. Jenkins, U. Schacht, A. McGrath, H. Berko, I. Schroder, R. Noble, T. Kuske, S. George, C. Heath, S. Zegelin, S. Curnow, H. Zhang, X. Sirault, J. Jimenez-Berni, and A. Hortle, 2014, An assessment of near surface CO_2 leakage detection techniques under Australian conditions: Energy Procedia, v. 63, p. 3891–3906, https://doi.org/10.1016/j.egypro.2014.11.419.

Harper, C.W., J.M. Blair, P.A. Fay, A.K. Knapp, and J.D. Carlisle, 2005, Increased rainfall variability and reduced rainfall amount decreases soil CO_2 flux in a grassland ecosystem: Global Change Biology, v. 11, no. 2, p. 322–334, https://doi.org/10.1111/j.1365-2486.2005.00899.x.

Howard, D.M., and P.J.A. Howard, 1993, Relationships between CO_2 evolution, moisture content and temperature for a range of soil types: Soil Biology and Biochemistry, v. 25, no. 11, p. 1537–1546, https://doi.org/10.1016/0038-0717(93)90008-Y.

Intergovernmental Panel on Climate Change, 2014, Climate change 2013—The physical science basis: Working Group I contribution to the fifth assessment report of the Intergovernmental Panel on Climate Change: Cambridge, UK, Cambridge University Press, https://doi.org/10.1017/CBO9781107415324.

Janssens, I.A., A.S. Kowalski, B. Longdoz, R. Ceulemans, 2000, Assessing forest

soil CO_2 efflux: An *in situ* comparison of four techniques: Tree Physiology, v. 20, no. 1, p. 23–32, https://doi.org/10.1093/treephys/20.1.23.

Korose, C.P., R.A. Locke II, C.S. Blakley, and C.H. Carman, 2014, Integration of near-surface monitoring information using ArcGIS at the Illinois Basin – Decatur Project, USA: Energy Procedia, v. 63, p. 3945–3955, https://doi.org/10.1016/j.egypro.2014.11.424.

Lewicki, J.L., G.E. Hilley, L. Dobeck, and L. Spangler, 2009, Dynamics of CO_2 fluxes and concentrations during a shallow subsurface CO_2 release: Environmental Earth Sciences, v. 60, no. 2, p. 285–297, https://www.osti.gov/servlets/purl/982055.

LI-COR Inc., 2015, Using the LI-8100A soil gas flux system & the LI-8150 multiplexer: Lincoln, Nebraska, LI-COR Biosciences, instruction manual, p. 52–63.

Madsen, R., L. Xu, B. Claassen, and D. McDermitt, 2009, Surface monitoring method for carbon capture and storage projects: Energy Procedia, v. 1, no. 1, p. 2161–2168, https://doi.org/10.1016/j.egypro.2009.01.281.

Midwest Geological Sequestration Consortium (MGSC), 2017, Home page, http://sequestration.org/ (accessed September 3, 2019).

Natural Resources Conservation Service, 2014, Web soil survey: Washington, DC, U.S. Department of Agriculture, Natural Resources Conservation Service, https://websoilsurvey.sc.egov.usda.gov/App/HomePage.htm (accessed September 3, 2019).

Raich, J.W., and C.S. Potter, 1995, Global patterns of carbon dioxide emissions from soils: Global Biogeochemical Cycles, v. 9, no. 1, p. 23–36, https://doi.org/10.1029/94GB02723.

Shepard, D., 1968, A two-dimensional interpolation function for irregularly-spaced data, *in* R.B. Blue Sr. and A.M. Rosenberg, eds., Proceedings of the 1968 23rd ACM National Conference, August 27–29, 1968, p. 517–524, https://dl.acm.org/citation.cfm?doid=800186.810616.

Singh, J.S., and S.R. Gupta, 1977, Plant decomposition and soil respiration in terrestrial ecosystems: The Botanical Review: v. 43, no. 4, p. 449–528, https://doi.org/10.1007/BF02860844.

Trimble, 2004, GPS Pathfinder® Systems: User Guide, Version 2.00, Revision A, Part Number 40889-10-ENG: Westminster, Colorado, Trimble Navigation Limited.

U.S. Environmental Protection Agency, 2009, Statistical analysis of groundwater monitoring data at RCRA facilities—Unified guidance: Washington, DC, U.S. Environmental Protection Agency, EPA 530/R-09-007, nepis.epa.gov (accessed September 23, 2019).

APPENDIX

Table A1 Flux ring installation locations, soil CO_2 flux averages, and number of measurements made at each location[1]

Label	Installation type	Longitude (DD)	Latitude (DD)	Average flux (μmol $m^{-2}s^{-1}$)	Count (*n*)
1A	Bare-shallow	–88.896992	39.880843	1.9	126
1B	Bare-shallow	–88.897001	39.880413	1.4	135
1C	Bare-shallow	–88.897006	39.879720	1.6	130
1D	Bare-shallow	–88.896995	39.879038	1.2	133
1E	Bare-shallow	–88.897000	39.878344	2.0	124
1F	Bare-shallow	–88.897002	39.877654	1.2	130
1G	Bare-shallow	–88.897002	39.876975	1.1	128
1H	Bare-shallow	–88.897004	39.876294	1.7	91
1I	Bare-shallow	–88.897004	39.875732	1.4	98
2A	Bare-shallow	–88.896108	39.881096	1.6	136
2B	Bare-shallow	–88.896108	39.880411	1.6	137
2C	Bare-shallow	–88.896110	39.879721	1.5	129
2D	Bare-shallow	–88.896107	39.879042	2.2	135
2E	Bare-shallow	–88.896107	39.878359	0.9	125
2F	Bare-shallow	–88.896108	39.877676	2.1	134
2G	Bare-shallow	–88.896101	39.876996	2.0	128
2H	Bare-shallow	–88.896100	39.876314	1.1	93
2I	Bare-shallow	–88.896094	39.875748	1.1	97
3A	Bare-shallow	–88.895220	39.881149	1.5	138
3B	Bare-shallow	–88.895216	39.880462	2.4	131
3C	Bare-shallow	–88.895217	39.879774	1.5	127
3D	Bare-shallow	–88.895223	39.879086	1.3	126
3E	Bare-shallow	–88.895225	39.878401	1.5	126
3F	Bare-shallow	–88.895222	39.877719	2.2	135
3G	Bare-shallow	–88.895224	39.877035	1.1	134
3H	Bare-shallow	–88.895232	39.876356	1.4	127
3I	Bare-shallow	–88.895237	39.875672	2.1	131
4A	Bare-shallow	–88.894326	39.881628	1.8	121
4B	Bare-shallow	–88.894330	39.881149	1.9	126
4C	Bare-shallow	–88.894331	39.880462	1.6	122
4D	Bare-shallow	–88.894334	39.879774	2.0	128
4E	Bare-shallow	–88.894342	39.879076	1.3	113
4F	Bare-shallow	–88.894347	39.878388	1.2	122
4G	Bare-shallow	–88.894353	39.877700	2.1	128
4H	Bare-shallow	–88.894342	39.877010	3.2	103
4I	Bare-shallow	–88.894313	39.876346	2.6	103
5A	Bare-shallow	–88.893431	39.881661	2.3	105
5B	Bare-shallow	–88.893431	39.881096	1.8	124
5C	Bare-shallow	–88.893427	39.880407	2.5	122
5D	Bare-shallow	–88.893431	39.879728	2.0	25

[1]DD, decimal degrees. Natural-shallow rings (pp. 26–27) include an “N” label, and bare-deep rings (p. 27) include a “D” label.

Continued on next page.

Table A1 *(Continued)*

Label	Installation type	Longitude (DD)	Latitude (DD)	Average flux (μmol $m^{-2}s^{-1}$)	Count (*n*)
5E	Bare-shallow	–88.893434	39.879041	1.4	16
5F	Bare-shallow	–88.893438	39.878359	1.6	122
5G	Bare-shallow	–88.893441	39.877675	2.9	126
5H	Bare-shallow	–88.893450	39.877429	6.7	114
6A	Bare-shallow	–88.892548	39.881691	2.2	120
6B	Bare-shallow	–88.892546	39.881100	1.9	112
6C	Bare-shallow	–88.892540	39.880415	1.5	119
6D	Bare-shallow	–88.892537	39.879728	1.7	130
6E	Bare-shallow	–88.892519	39.879044	1.8	108
7A	Bare-shallow	–88.891653	39.881396	2.0	122
7B	Bare-shallow	–88.891653	39.881094	2.6	124
7C	Bare-shallow	–88.891648	39.880399	1.3	120
7D	Bare-shallow	–88.891644	39.879990	1.9	125
8A	Bare-shallow	–88.890744	39.881738	2.4	121
8B	Bare-shallow	–88.890756	39.881081	2.2	122
8C	Bare-shallow	–88.890772	39.880397	1.4	115
8D	Bare-shallow	–88.890778	39.880017	1.5	115
9A	Bare-shallow	–88.889878	39.881759	1.6	123
9B	Bare-shallow	–88.889878	39.881089	1.7	121
9C	Bare-shallow	–88.889875	39.880370	1.7	101
10A	Bare-shallow	–88.892995	39.877575	3.6	115
10B	Bare-shallow	–88.893439	39.877561	1.9	93
10C	Bare-shallow	–88.893901	39.877550	1.8	112
10D	Bare-shallow	–88.894358	39.877527	2.7	105
10E	Bare-shallow	–88.894485	39.877425	1.6	105
10F	Bare-shallow	–88.894492	39.877081	2.1	109
10G	Bare-shallow	–88.894508	39.876746	2.0	107
10H	Bare-shallow	–88.894501	39.876400	2.3	102
10I	Bare-shallow	–88.894206	39.876205	2.5	108
10J	Bare-shallow	–88.893772	39.876129	1.9	105
10K	Bare-shallow	–88.893333	39.876079	2.7	104
10L	Bare-shallow	–88.892897	39.876124	2.8	105
11A	Bare-shallow	–88.892976	39.877334	1.0	93
11B	Bare-shallow	–88.893424	39.877324	1.6	91
11C	Bare-shallow	–88.893836	39.877317	1.8	91
11D	Bare-shallow	–88.894137	39.877303	1.3	88
11E	Bare-shallow	–88.894152	39.876997	1.4	87
11F	Bare-shallow	–88.894154	39.876609	1.4	86
11G	Bare-shallow	–88.894124	39.876474	2.0	95
11H	Bare-shallow	–88.893670	39.876433	2.5	97
11I	Bare-shallow	–88.893226	39.876447	3.6	91
1AN	Natural-shallow	–88.896984	39.880815	6.1	132
1CN	Natural-shallow	–88.896998	39.879704	7.0	126
1EN	Natural-shallow	–88.896988	39.878320	5.8	132
1GN	Natural-shallow	–88.896994	39.876954	4.6	128
1IN	Natural-shallow	–88.896997	39.875759	3.7	94

Continued on next page.

Table A1 *(Continued)*

Label	Installation type	Longitude (DD)	Latitude (DD)	Average flux (μmol $m^{-2}s^{-1}$)	Count (*n*)
2BN	Natural-shallow	–88.896098	39.880373	4.2	136
2DN	Natural-shallow	–88.896095	39.879010	5.4	133
2FN	Natural-shallow	–88.896103	39.877649	3.5	130
2HN	Natural-shallow	–88.896092	39.876282	3.8	91
3AN	Natural-shallow	–88.895211	39.881122	4.9	125
3CN	Natural-shallow	–88.895212	39.879745	4.8	127
3EN	Natural-shallow	–88.895217	39.878374	4.2	126
3GN	Natural-shallow	–88.895219	39.877002	5.8	126
3IN	Natural-shallow	–88.895232	39.875639	6.5	120
4AN	Natural-shallow	–88.894333	39.881649	4.7	99
4CN	Natural-shallow	–88.894331	39.880430	5.3	123
4EN	Natural-shallow	–88.894339	39.879046	4.2	116
4GN	Natural-shallow	–88.894343	39.877671	5.4	122
5BN	Natural-shallow	–88.893427	39.881070	5.2	118
5CN	Natural-shallow	–88.893426	39.880380	5.6	95
5DN	Natural-shallow	–88.893430	39.879699	6.4	20
5FN	Natural-shallow	–88.893440	39.878330	5.0	119
6AN	Natural-shallow	–88.892553	39.881701	5.3	97
6CN	Natural-shallow	–88.892533	39.880389	4.8	117
6EN	Natural-shallow	–88.892510	39.879017	4.5	117
7BN	Natural-shallow	–88.891659	39.881070	5.7	107
7DN	Natural-shallow	–88.891645	39.879963	5.2	103
8AN	Natural-shallow	–88.890743	39.881708	4.8	97
8CN	Natural-shallow	–88.890766	39.880369	3.1	111
9BN	Natural-shallow	–88.889875	39.881061	6.3	110
3AD	Bare-deep	–88.895214	39.881149	1.8	122
4CD	Bare-deep	–88.894334	39.880458	1.8	80
4ED	Bare-deep	–88.894337	39.879077	1.4	97
5DD	Bare-deep	–88.893427	39.879729	2.5	14
6CD	Bare-deep	–88.892537	39.880418	1.6	73
6ED	Bare-deep	–88.892513	39.879049	1.6	96